CHALMERS
UNIVERSITY OF TECHNOLOGY

Robust Analog Beamforming for Periodic Broadcast V2V Communication

Citation for the original published paper (version of record):
Bencheikh Lehocine, C., Brännström, F., Ström, E. (2022). Robust Analog Beamforming for Periodic Broadcast V2V Communication. IEEE Transactions on Intelligent Transportation Systems, 23(10): 18404-18422. http://dx.doi.org/10.1109/TITS.2022.3161045

Robust Analog Beamforming for Periodic Broadcast V2V Communication

Chouaib Bencheikh Lehocine, Fredrik Brännström, and Erik G. Ström, *Fellow, IEEE*

***Abstract*—We generalize an existing low-cost analog signal processing concept that takes advantage of the periodicity of vehicle-to-vehicle broadcast service to the transmitter side. In particular, we propose to process multiple antennas using either an analog beamforming network (ABN) of phase shifters, or an antenna switching network (ASN) that periodically alternates between the available antennas, to transmit periodic messages to receivers that have an analog combining network (ACN) of phase shifters, which has been proposed in earlier work. To guarantee robustness, we aim to minimize the burst error probability for the worst receiving vehicular user, in a scenario of bad propagation condition that is modeled by a single dominant path between the communicating vehicles. In absence of any form of channel knowledge, we analytically derive the optimal parameters of both ABN and ASN. The ABN beamforming vector is found to be optimal for all users and not only for the worst receiving user. Further, we demonstrate that Alamouti scheme for the special case of two transmit antennas yields similar performance to ABN and ASN. At last, we show that the derived parameters of the two proposed transmission strategies are also optimal when hybrid ACN-maximal ratio combining is used at the receiver.**

***Index Terms*—Broadcast Vehicle-to-Vehicle communication, periodic communication, beamforming.**

I. Introduction

VEHICULAR communication paves the path for the realization of cooperative intelligent transportation systems (C-ITS). By allowing vehicles to share real-time information about their status, vehicles can cooperate and coordinate their movement and maneuvers, which results in increased safety, efficiency, comfort, and sustainability of transportation systems. Since C-ITS require the exchange of time-sensitive, critical information, very high reliability and low latency need to be supported by the vehicular communication systems. One typical technical solution to those requirements is the use of multiple antenna systems. In the context of vehicular communications, antennas pose their own challenges. It has been noted in several studies, including [1]–[3], that antenna patterns are distorted by several factors including vehicle body and mounting position. Such distortions can lead to very low gains or even blind spots in certain directions, which may result in low performance or outage when the transmitted or received signal is along those directions. To enable robust vehicle-to-vehicle (V2V) communication against the effects of such disturbances, multiple antennas can be processed with the objective of ensuring certain performance in the worst-case propagation scenario with respect to the antenna system.

The analog combining network (ACN) proposed in [4], is such a solution that was designed to combine antennas at the receiver to achieve robustness. In particular, it was designed to minimize the outage probability of a C-ITS application, measured through the loss of K consecutive periodic status messages, when the received signal coincides with the worst-case angle of arrival (AOA). We note that this metric is related to age-of-information (AoI) assessment metric of broadcast periodic communication [5], defined as the age of the information contained in the last correctly received periodic message. The ACN is based on pure analog combining. To leverage the digital processing benefits, a hybrid analog-digital solution was presented in our previous work [6]. In both [4] and [6], the transmitter side has not been considered. For a comprehensive multiple antenna system, we would like to explore, in accordance with a receiver that uses an ACN, what beamforming solutions can be used at the transmitter side to improve robustness in a scenario of V2V communication. As we are considering a broadcast transmission, feeding back the channel state information (CSI) may be infeasible due to the high number of vehicular users (VUs). In addition, every VU has only a limited number of antennas and limited processing capabilities to beamform, based on CSI, to all receiving VUs at the same time. Therefore, we herein target a transmit beamformer that does not depend on CSI. This implies a low-complexity solution. Moreover, we target a low-cost analog beamforming solution.

A selection of publications that are relevant to the scope of our work is [7]–[10]. In [7], two transmission strategies were proposed and evaluated through measurement in a platoon scenario. The first strategy is based on alternating the transmit antennas periodically. The second uses information about the road curvature and selects the antenna with a higher probability to have a line of sight (LOS) with the receiving antennas. The authors assess both strategies using an AoI approach. The proposed schemes consider only the platoon vehicles. Other vehicles on the road, to which cooperative messages have to reach, are not considered. Similarly to [7], in [8], an antenna selection technique was proposed and evaluated using simulations in a platoon scenario. To perform antenna selection, VUs send feedback to the network, notifying about their antenna capabilities, the type of message to be sent, road conditions (e.g., position of surrounding vehicles), and radio channel conditions (e.g., received power on each antenna). Then, the network selects a subset of antennas that is most suitable for the communication context identified from the feedback. This technique is feasible only under network coverage. VUs that

This research has been carried out in the antenna systems center *ChaseOn* in a project financed by Swedish Governmental Agency of Innovation Systems (Vinnova), Chalmers, Bluetest, Ericsson, Keysight, RISE, Smarteq, and Volvo Cars.

The authors are with the Communication Systems Group, Department of Electrical Engineering, Chalmers University of Technology, 412 96 Gothenburg, Sweden (e-mail: chouaib@chalmers.se; fredrik.brannstrom@chalmers.se; erik.strom@chalmers.se)

are out of coverage can not benefit from it. Therefore, in this work, we aim for a solution that does not rely on network coverage or feedback. In [9], another transmit beamforming structure based on switches is proposed. The scheme is fully analog, and it is a variant of antenna selection. Instead of selecting a single antenna element, the transmitter chooses a subset of antennas that result in maximizing the signal-to-noise ratio (SNR) at the receiver. However, the scheme relies on CSI, and as explained earlier, for our scenario of broadcast transmission such an approach is not very relevant. Another work of interest is a random beamforming technique proposed in [10]. A uniform linear array of antennas is weighed by a vector that is randomized over time-frequency blocks. The achieved average pattern over many time-frequency blocks is omnidirectional. This scheme does not require channel knowledge, but it uses several radio frequency (RF) chains, and therefore it is a digital strategy. Besides this, standard digital approaches that do not depend on CSI, e.g., Alamouti transmit diversity [11], and similar space-time or space-frequency codes, are relevant in this scenario, however, they require the use of multiple RF chains. We are interested in finding out how we can improve the system in the analog domain, which is characterized by low cost. The digital solutions can be used on top to give enhanced performance and hybrid structures that achieve a trade-off between performance and cost.

In this paper, we assume that VUs use an analog combining network as proposed in [4] at the receiver, while we propose two strategies that do not rely on CSI at the transmitter. The first one is an analog beamforming network (ABN) of phase shifters that has a similar construction to the receiver ACN. The second strategy is an antenna switching network (ASN) and it is based on alternating between the transmit antennas in a periodic manner. We note that this switching approach was used in [7] as well, however, it did not take into account a receiver structure as the one proposed here. Furthermore, it was assessed using AoI which is related to, but not the same as our assessment metric. Given the proposed schemes, we optimize the overall system parameters at both transmitter and receiver for the ABN, while for the ASN only the receiver parameters are optimized. Our optimization is based on the minimization of burst error probability (BrEP) of K consecutive packets for the worst user in the system i.e., the user experiencing the worst BrEP, which under some assumptions, can be defined by the worst-case AOA and angle of departure (AOD). That ensures robust communication against unfavorable angles with respect to the antenna system. Once the optimal parameters are found, we come to show that the developed networks can be further improved by adding a digital processing stage at the receiver in the form of a hybrid combiner with a similar structure to [6]. A summary of the contributions of this paper follows.

- We present two fully analog transmission strategies (ABN and ASN) that do not require any channel knowledge, in combination with an ACN at the receiver.
- We provide the optimal transmitter and receiver parameters (phase slopes) associated with both strategies. These parameters minimize the BrEP for the worst receiving VU, under certain assumptions.
- We extend the optimality proof of the phase slopes of the ACN developed in [4]. The phase slopes were shown to be optimal only for systems with a number of receive antennas $L_{\mathrm{r}} \in \{2, 3\}, L_{\mathrm{r}} \leq K$. Here, we demonstrate that they are optimal for any system with $L_{\mathrm{r}} \leq K$.
- We demonstrate that the analog structures can be upgraded by a digital processing stage at the receiver, based on maximal ratio combining (MRC), to yield enhanced performance.

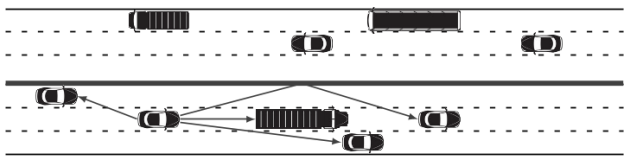

Fig. 1. CAM broadcasting in a highway scenario. Only the dominant path, LOS or SBR between the transmitting and receiving vehicles is shown. The concrete wall or metallic fence separating the two driving directions is an example of a reflecting object.

II. System Model

In this section, we present the system model and the transmission strategies we are considering together with the receiver structure. Moreover, we state the main assumptions that we use to deduce the optimal parameters of the proposed strategies.

A. Antennas and Channel Model

Scarce multipath propagation with a single dominant component—LOS or SBR—between the communicating vehicles (see Fig. 1), poses a challenging scenario for the robustness of a V2V communication based on some antenna system. In such a scenario, the AOD and AOA may coincide with a very low gain of the antenna patterns, which can lead to packet loss, or outage if the same directions are approximately sustained for a time span of several consecutive packets. Such propagation conditions have been noted to be prominent in traffic scenarios where the road is not surrounded by buildings [12], e.g., highway. Moreover, it has been noted that in such propagation environments the azimuth angular spread is small [12], which implies that the few existing multipath components are restricted to a narrow sector of the antenna system. Therefore, a good framework to ensure robust V2V communication against unfavorable AOD and AOA is to use a channel model that assumes such propagation conditions. In the model to follow, however, we consider only the dominant path between the communicating vehicles, since it contributes to most of the received power. Let g_m^{s} and g_l^{r} be the far field functions of the m^{th} transmit and l^{th} receive antennas[1], respectively. The antennas are vertically polarized. We assume that the far field functions are measured such that the antenna position, placement, and car body effects are taken into account, e.g., for side-windows mounted antennas, the

[1]Throughout the paper, the superscript letter 's' stands for sender, while 'r' stands for receiver.

blockage created by the vehicle body is accounted for in the far field functions. Then, the baseband channel gain between transmitter (Tx) antenna m and receiver (Rx) antenna l can be modeled as [13, Ch. 6]

$$h_{l,m}(t) = a(t) g_m^{\mathrm{s}}(\phi^{\mathrm{s}}, \theta^{\mathrm{s}}) g_l^{\mathrm{r}}(\phi^{\mathrm{r}}, \theta^{\mathrm{r}}) \mathrm{e}^{\jmath \Omega_m^{\mathrm{s}}} \mathrm{e}^{-\jmath \Omega_l^{\mathrm{r}}}, \quad (1)$$

where $a(t) = |a(t)| \mathrm{e}^{-\jmath 2\pi f_{\mathrm{c}} \tau_0(t)}$ is the complex-amplitude of the dominant component, f_{c} is the carrier frequency, $\tau_0(t) = d_{0,0}(t)/c$, $d_{0,0}(t)$ is the physical path length between the transmit and receive reference antenna pair $(0, 0)$, and c is the speed of light in free space. The AOD and AOA in the azimuth and elevation planes are denoted by $(\phi^{\mathrm{s}}, \theta^{\mathrm{s}})$ and $(\phi^{\mathrm{r}}, \theta^{\mathrm{r}})$, respectively. The relative phase shifts with respect to the reference antennas, Ω_m^{s}, Ω_l^{r}, depend on the AOD and AOA and they are given by [13, Ch. 6]

$$\Omega_m^{\mathrm{s}} = \langle \boldsymbol{k}_{\mathrm{c}}(\phi^{\mathrm{s}}, \theta^{\mathrm{s}}), \boldsymbol{u}_m^{\mathrm{s}} - \boldsymbol{u}_0^{\mathrm{s}} \rangle, \quad (2)$$

$$\Omega_l^{\mathrm{r}} = \langle \boldsymbol{k}_{\mathrm{c}}(\phi^{\mathrm{r}}, \theta^{\mathrm{r}}), \ \boldsymbol{u}_l^{\mathrm{r}} - \boldsymbol{u}_0^{\mathrm{r}} \rangle, \quad (3)$$

where $\langle \cdot, \cdot \rangle$ denotes the inner product, $\boldsymbol{u}_m^{\mathrm{s}}$ and $\boldsymbol{u}_l^{\mathrm{r}}$ are the coordinates of m^{th} transmit and l^{th} receive antennas respectively, and $\boldsymbol{k}_{\mathrm{c}}(.)$ is the unit wave vector in the direction of AOD or AOA, with coordinates $(k_{\mathrm{x}}, k_{\mathrm{y}}, k_{\mathrm{z}}) = 2\pi/\lambda_{\mathrm{c}}(\sin(\theta)\cos(\phi), \sin(\theta)\sin(\phi), \cos(\theta))$. The elevation plane angle θ is here defined as the angle between the z-axis and the vector of interest (i.e., polar angle).

We note that in (1), $a(t)$, $(\phi^{\mathrm{s}}, \theta^{\mathrm{s}})$, and $(\phi^{\mathrm{r}}, \theta^{\mathrm{r}})$ are assumed to be the same for all antenna pairs (l, m). This assumption is reasonable when the distance between the Tx and Rx, or the distance separating the refection point and the antenna arrays (SBR propagation), is much larger than the inter-separation between antenna elements of both Tx and Rx arrays [14, Ch. 7]. Furthermore, the relative phase differences as expressed in (2) and (3) follow from the same assumption. Besides this, it is worth noting that the channel model is not restricted to a specific antenna array arrangement.

Taking into account that vehicles are relatively of the same height, the elevation angles are restricted to a narrow sector, and they are therefore of less importance compared to the azimuth angles in a scenario of V2V communication. Following that, we assume that the dominant component is arriving along the azimuth plane with $\theta^{\mathrm{s}} \approx \pi/2$, $\theta^{\mathrm{r}} \approx \pi/2$. Consequently, the AOD and AOA can be restricted to the azimuth plane angles ϕ^{s} and ϕ^{r} in (1) and the far field functions are expressed as

$$g_m^{\mathrm{s}}(\phi^{\mathrm{s}}) \triangleq g_m^{\mathrm{s}}(\phi^{\mathrm{s}}, \pi/2), \quad g_l^{\mathrm{r}}(\phi^{\mathrm{r}}) \triangleq g_l^{\mathrm{r}}(\phi^{\mathrm{r}}, \pi/2). \quad (4)$$

B. Traffic Model of IEEE802.11p Cooperative Service

Consider a scenario where vehicles periodically broadcast their status information to all vehicles in their proximity to create a cooperative environment. Such functionality can be supported by IEEE802.11p V2X technology, where vehicles broadcast a CAM every T s that include information about their dynamic status, like position, speed, heading, etc. The period of dissemination is specified to be in the range of $0.1 \leq T \leq 1$ s [15]. The physical layer supports multiple data rates, however, for CAMs a data rate of 6 Mbit/s is deemed suitable [16]. Given that a reasonable CAM size is in the range 100 to 500 bytes [16], the message duration $T_{\mathrm{m}} < 0.7$ ms.

Motivated by the high dissemination frequency of CAMs, it has been suggested in several works including [5], to measure the reliability of a C-ITS application that depends on their content using AoI. In this framework, given that a packet is generated by a vehicle at time $t = 0$, then transmitted and correctly received at time $t = \tau$ by a receiving vehicle, if the time elapsing until the next packet reception exceeds a maximum allowable age $A_{\max}$, then an outage is declared. Exceeding $A_{\max}$ implies that the age of the status information decoded at $t = \tau$ is outdated and cannot be used by a C-ITS application at the receiving vehicle. If the latency between the generation and reception of packets is neglected (i.e, $\tau \approx 0$), age-of-information is equivalent to inter-reception time (IRT) which is defined as the time separating two successful reception of packets, and it is elaborated in [17]. BrEP defined as the probability of losing K consecutive CAMs can be thought of as a physical layer counterpart to AoI and it was first proposed in [4]. If latency is neglected, the two parameters can be related as $A_{\max} = KT$ where K is the burst length and T is the period of dissemination.

C. Transmission Strategies

In the following, we assume that a reference transmitting vehicle is equipped with L_{s} antennas and the receiving vehicles are equipped with L_{r} antennas. The receiver structure is based on an ACN as proposed in [4]. The combining network does not depend on CSI, and it is composed of phase shifters that are modeled as affine functions of time according to $\varphi_l^{\mathrm{r}} = (\alpha_l^{\mathrm{r}} t + \beta_l^{\mathrm{r}})$, where $\alpha_l^{\mathrm{r}} \in \mathbb{R}$ represents a phase slope, $\beta_l^{\mathrm{r}} \in [0, 2\pi)$ is an unknown initial phase offset, and $0 \leq l \leq L_{\mathrm{r}} - 1$. We are interested in finding the optimal parameters of the network for two multiple antenna beamforming strategies. Before presenting the strategies, we develop simple, generic equations for the received signal of a particular VU. Let $\boldsymbol{b}$ be the beamforming vector, the received signal can be expressed as

$$\boldsymbol{r} = a(t) \boldsymbol{H} \boldsymbol{b} x(t) + \boldsymbol{n}, \quad (5)$$

where $x(t) = \tilde{x}(t - \tau_0(t))$, $\tilde{x}(t)$ is the transmitted baseband signal, and $\tau_0(t)$ is the propagation delay. The channel matrix $\boldsymbol{H}$ has entries $[\boldsymbol{H}]_{l,m} = h_{l,m}(t)/a(t)$ following (1). The noise vector $\boldsymbol{n}$ has L_{r} elements, each modeled as independent white Gaussian noise over the system bandwidth with $\mathcal{CN}(0, \sigma_{\mathrm{n}}^2)$. At the receiver, we apply the analog combining vector $\boldsymbol{w}$,

$$[\boldsymbol{w}]_l = \mathrm{e}^{-\jmath(\alpha_l^{\mathrm{r}} t + \beta_l^{\mathrm{r}})}, \quad 0 \leq l \leq L_{\mathrm{r}} - 1. \quad (6)$$

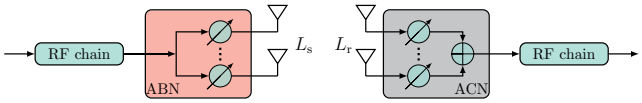

(a) Analog beamforming network of phase shifters (ABN)

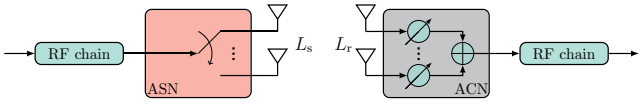

(b) Transmit antenna switching network (ASN)

Fig. 2. Transmission strategies structures.

The combined signal is given by

$$r(t) = a(t)x(t)\boldsymbol{w}^{\mathsf{H}}\boldsymbol{H}\boldsymbol{b} + \boldsymbol{w}^{\mathsf{H}}\boldsymbol{n} \tag{7}$$

$$= a(t)x(t)c(t) + \tilde{n}(t), \tag{8}$$

where $c(t) = \boldsymbol{w}^{\mathsf{H}}\boldsymbol{H}\boldsymbol{b}$ and $\tilde{n}(t) = \boldsymbol{w}^{\mathsf{H}}\boldsymbol{n}$ denote the effective channel gain and noise at the output of the ACN. The signal $\tilde{n}(t)$ is a zero-mean white Gaussian noise with $P_{\mathrm{n}} = \mathbb{E}\{|\boldsymbol{w}^{\mathsf{H}}\boldsymbol{n}|^2\} = L_{\mathrm{r}}\sigma_{\mathrm{n}}^2$, and $P_{\mathrm{r}} = \mathbb{E}\{|a(t)x(t)|^2\}$ is the average received power. In the following, we present the two beamforming strategies and their corresponding effective channel gains.

1) ABN of Phase Shifters: We propose a transmitter structure that is similar to the receiver combining technique. Namely, we use phase shifters modeled as $\varphi_m^{\mathrm{s}}(t) = (\alpha_m^{\mathrm{s}} t + \beta_m^{\mathrm{s}})$ per antenna branch $0 \le m \le L_{\mathrm{s}} - 1$, where $\alpha_m^{\mathrm{s}} \in \mathbb{R}$ is a phase slope and $\beta_m^{\mathrm{s}} \in [0, 2\pi)$ is an unknown initial phase offset. The overall structure is shown in Fig. 2(a). The analog beamforming vector is given by

$$[\boldsymbol{b}]_m = \frac{1}{\sqrt{L_{\mathrm{s}}}} \mathrm{e}^{\jmath(\alpha_m^{\mathrm{s}} t + \beta_m^{\mathrm{s}})}, \quad 0 \le m \le L_{\mathrm{s}} - 1. \tag{9}$$

Note that the beamforming vector is determined by the phase slopes ($\{\beta_m^{\mathrm{s}}\}$ are unknown and could take any value in $[0, 2\pi)$). The factor $1/\sqrt{L_{\mathrm{s}}}$, comes from splitting equally the power among the transmit antenna branches, which is a reasonable measure in absence of channel knowledge. Also, it ensures the use of a similar power level compared to the single transmit antenna case. Using (1), (4), and (8) the corresponding effective channel gain is given by

$$c^{(\mathrm{a})}(t) = \frac{1}{\sqrt{L_{\mathrm{s}}}} \sum_{m=0}^{L_{\mathrm{s}}-1} g_m^{\mathrm{s}}(\phi^{\mathrm{s}}) \mathrm{e}^{-\jmath(-\Omega_m^{\mathrm{s}} - \alpha_m^{\mathrm{s}} t - \beta_m^{\mathrm{s}})} \times \sum_{l=0}^{L_{\mathrm{r}}-1} g_l^{\mathrm{r}}(\phi^{\mathrm{r}}) \mathrm{e}^{-\jmath(\Omega_l^{\mathrm{r}} - \alpha_l^{\mathrm{r}} t - \beta_l^{\mathrm{r}})}. \tag{10}$$

2) Transmit ASN: Instead of using analog phase shifters, we consider a transmitter that uses only switches. Since we are restricting any form of channel-based control of the switches, an ASN uses a single antenna element for transmission then switches to the next element for the next transmission. The overall structure is illustrated in Fig. 2(b). Let k denote the packet index, the ASN beamforming vector for $kT \le t \le kT + T_{\mathrm{m}}$, can be expressed as

$$[\boldsymbol{b}]_m = 1, \quad m = \mathrm{mod}(k, L_{\mathrm{s}}) \tag{11}$$

$$[\boldsymbol{b}]_i = 0, \quad \forall i \neq m$$

where $\mathrm{mod}(a, b)$ denotes the remainder of dividing a by b. We note that the same antenna element is used periodically for every L_{s} transmissions. The received signal following this strategy for the k^{th} packet is given by (8), with effective channel gain at $kT \le t \le kT + T_{\mathrm{m}}$

$$c^{(\mathrm{b})}(t) = g_m^{\mathrm{s}}(\phi^{\mathrm{s}}) \mathrm{e}^{\jmath\Omega_m^{\mathrm{s}}} \sum_{l=0}^{L_{\mathrm{r}}-1} g_l^{\mathrm{r}}(\phi^{\mathrm{r}}) \mathrm{e}^{-\jmath(\Omega_l^{\mathrm{r}} - \alpha_l^{\mathrm{r}} t - \beta_l^{\mathrm{r}})}, \tag{12}$$

where $m = \mathrm{mod}(k, L_{\mathrm{s}})$. Note that the power of the signal is not split in this case, and a single antenna element uses full power for every transmission.

D. Assumptions

Before tackling the design task, we consider a number of assumptions. First, since the packet duration is very small in comparison to the period, $T_{\mathrm{m}} \ll T$, we assume that the effective channel gains are constant over the packet duration for both strategies. That is

$$c^{(.)}(t) \approx c^{(.)}(kT), \quad kT \le t \le kT + T_{\mathrm{m}}. \tag{13}$$

Second, given the channel model, if the AOD and AOA coincide with directions along which the antenna systems have low gain, and the directions are sustained for KT s then an outage may occur. Thus, taking into account this worst-case propagation scenario and as part of our robust design approach, we assume that the position and speed of transmitting and receiving vehicles, and potential reflecting objects are such that the dominant component between the Tx and Rx experiences negligible change over the duration of KT s. Consequently, the following assumptions apply.

- The AOD, ϕ^{s}, and AOA, ϕ^{r}, are assumed to experience negligible change and thus are modeled as constant over the duration of KT s.
- From (2) and (3), we see that Ω_m^{s} and Ω_l^{r} depend on the AOD, AOA, and the geometry of the antenna arrays (which is fixed), therefore they can be assumed constant over the duration of KT s as well.
- The average received power along the dominant component expressed as $P_{\mathrm{r}} = \mathbb{E}\{|a(t)x(t)|^2\}$ is assumed constant over KT s.

III. Design of the Tx-Rx Schemes

There exist several users to which CAM messages need to reach. From a robustness aspect, we want to ensure certain performance for the worst receiving VU. That depends on the applied beamforming vector $\boldsymbol{b}$, the combining vector $\boldsymbol{w}$, and the channel between the transmitting and receiving VUs. For our simplified model, the channel can be represented by the AOD, AOA, and the far field functions of antennas. Assuming that all receiving VUs have the same antenna system, (i.e., the same number of antennas L_{r}, and the same far field functions g_l^{r}), the worst receiving user is defined by the worst-case AOD, AOA for a given $\boldsymbol{b}$ and $\boldsymbol{w}$. We will find out later that the solution found under this assumption, is also optimal when the system is generalized to receiving users with different numbers of antennas and different far field functions.

We did set our framework to ensure the robustness of the system. To quantify performance, we use the concept of BrEP, that is, the probability of losing K consecutive CAM packets. To derive some analytical results, we resort to the following two assumptions. First, in our considered propagation scenario of scarce multipath with a dominant component, the strongest tap in a discrete baseband channel model has been observed to follow a Rician distribution with a κ-factor that is medium to high (5.71 to 16.51 dB corresponding to obstructed LOS and LOS conditions, respectively) [18]. A Rician channel will tend to an additive white Gaussian noise (AWGN) channel with increasing κ-factor, and the resulting packet error probability can be well approximated by an exponential function of SNR

$$J_{\mathrm{a}}(\phi^{\mathrm{r}},\phi^{\mathrm{s}},\boldsymbol{\alpha}^{\mathrm{r}},\boldsymbol{\alpha}^{\mathrm{s}},\boldsymbol{\psi}^{\mathrm{r}},\boldsymbol{\psi}^{\mathrm{s}}) = \sum_{l=0}^{L_{\mathrm{r}}-2}\sum_{i=l+1}^{L_{\mathrm{r}}-1} c_{l,i}(\phi^{\mathrm{r}},\phi^{\mathrm{s}}) \sum_{k=0}^{K-1}\cos\left(\Delta\psi_{l,i}^{\mathrm{r}} - \Delta\alpha_{l,i}^{\mathrm{r}}kT\right)$$
$$+ \sum_{m=0}^{L_{\mathrm{s}}-2}\sum_{j=m+1}^{L_{\mathrm{s}}-1} d_{m,j}(\phi^{\mathrm{r}},\phi^{\mathrm{s}}) \sum_{k=0}^{K-1}\cos\left(\Delta\psi_{m,j}^{\mathrm{s}} - \Delta\alpha_{m,j}^{\mathrm{s}}kT\right)$$
$$+ \sum_{l=0}^{L_{\mathrm{r}}-2}\sum_{i=l+1}^{L_{\mathrm{r}}-1}\sum_{m=0}^{L_{\mathrm{s}}-2}\sum_{j=m+1}^{L_{\mathrm{s}}-1} c'_{l,i}(\phi^{\mathrm{r}})d'_{m,j}(\phi^{\mathrm{s}}) \sum_{k=0}^{K-1}\cos\left(\Delta\psi_{l,i}^{\mathrm{r}} - \Delta\alpha_{l,i}^{\mathrm{r}}kT\right)\cos\left(\Delta\psi_{m,j}^{\mathrm{s}} - \Delta\alpha_{m,j}^{\mathrm{s}}kT\right). \quad (25)$$

$$c_{l,i}(\phi^{\mathrm{r}},\phi^{\mathrm{s}}) = \left(\sum_{m=0}^{L_{\mathrm{s}}-1}\frac{|g_m^{\mathrm{s}}(\phi^{\mathrm{s}})|^2}{L_{\mathrm{s}}}\right)\overbrace{2\frac{|g_l^{\mathrm{r}}(\phi^{\mathrm{r}})||g_i^{\mathrm{r}}(\phi^{\mathrm{r}})|}{L_{\mathrm{r}}}}^{c'_{l,i}(\phi^{\mathrm{r}})}, \qquad d_{m,j}(\phi^{\mathrm{r}},\phi^{\mathrm{s}}) = \left(\sum_{l=0}^{L_{\mathrm{r}}-1}\frac{|g_l^{\mathrm{r}}(\phi^{\mathrm{r}})|^2}{L_{\mathrm{r}}}\right)\overbrace{2\frac{|g_m^{\mathrm{s}}(\phi^{\mathrm{s}})||g_j^{\mathrm{s}}(\phi^{\mathrm{s}})|}{L_{\mathrm{s}}}}^{d'_{m,j}(\phi^{\mathrm{s}})}. \quad (26)$$

in this case [19]. Thus, in the following, we assume that the packet error probability is an exponential function of SNR. Second, interference from other vehicles and potential packet collisions are not considered[2] in our scenario (ideal medium access control is assumed). Thus, packet errors occur solely due to noise and propagation and they are, therefore, assumed to be independent. Under these two assumptions, the minimization of BrEP is equivalent to the maximization of the sum of the SNR of the K packets, referred to as sum-SNR in this work. Exact details of relating BrEP to sum-SNR can be found in [4, Section III], [6, Section III.B].

In summary, under the assumptions introduced herein, the design objective, which can be formulated as minimizing BrEP of K packets for the worst receiving VU, is equivalent to maximizing the sum-SNR of K packets for the worst-case AOA and AOD. From here, we go through the design procedure for the two schemes separately.

A. Design of the Analog Beamforming Network

1) Deriving the SNR per Packet: Given an ABN transmitter, the received signal is modeled by (8), where the effective channel gain is given by $c^{(\mathrm{a})}$ (10). Incorporating the assumptions in Section II-D, $c^{(\mathrm{a})}$ can be approximated when $kT \le t \le kT + T_{\mathrm{m}}$ as

$$c^{(\mathrm{a})}(kT) = \frac{1}{\sqrt{L_{\mathrm{s}}}}\sum_{m=0}^{L_{\mathrm{s}}-1}|g_m^{\mathrm{s}}(\phi^{\mathrm{s}})|\mathrm{e}^{-\jmath(\psi_m^{\mathrm{s}}-\alpha_m^{\mathrm{s}}kT)} \times \sum_{l=0}^{L_{\mathrm{r}}-1}|g_l^{\mathrm{r}}(\phi^{\mathrm{r}})|\mathrm{e}^{-\jmath(\psi_l^{\mathrm{r}}-\alpha_l^{\mathrm{r}}kT)}, \quad (14)$$

where the effective channel phases are given by

$$\psi_m^{\mathrm{s}} = \mathrm{mod}\left(-\Omega_m^{\mathrm{s}} - \underbrace{\angle g_m^{\mathrm{s}}(\phi^{\mathrm{s}})}_{} - \beta_m^{\mathrm{s}}, 2\pi\right), \quad (15)$$
$$\psi_l^{\mathrm{r}} = \mathrm{mod}\left(\Omega_l^{\mathrm{r}} - \underbrace{\angle g_l^{\mathrm{r}}(\phi^{\mathrm{r}})}_{} - \beta_l^{\mathrm{r}}, 2\pi\right), \quad (16)$$

and they are approximately constant over KT s. Let $\boldsymbol{\psi}^{\mathrm{r}}$, $\boldsymbol{\alpha}^{\mathrm{r}}$ be L_{r}-vectors with entries corresponding to ψ_l^{r} and α_l^{r}, respectively, and analogously are defined the L_{s}-vectors $\boldsymbol{\psi}^{\mathrm{s}}$ and $\boldsymbol{\alpha}^{\mathrm{s}}$. Then, recalling (8) we can express the k^{th} packet SNR, for $k = 0, 1, \cdots, K-1$ as

$$\gamma_k^{(\mathrm{a})} = \frac{P_{\mathrm{r}}}{L_{\mathrm{r}}\sigma_{\mathrm{n}}^2}|c^{(\mathrm{a})}(kT)|^2 \quad (17)$$
$$= \frac{P_{\mathrm{r}}}{\sigma_{\mathrm{n}}^2}\frac{G_{\mathrm{r}}(\phi^{\mathrm{r}},\boldsymbol{\alpha}^{\mathrm{r}},\boldsymbol{\psi}^{\mathrm{r}},k)}{L_{\mathrm{r}}}\frac{G_{\mathrm{s}}(\phi^{\mathrm{s}},\boldsymbol{\alpha}^{\mathrm{s}},\boldsymbol{\psi}^{\mathrm{s}},k)}{L_{\mathrm{s}}}, \quad (18)$$

where

$$G_{\mathrm{r}}(\phi^{\mathrm{r}},\boldsymbol{\alpha}^{\mathrm{r}},\boldsymbol{\psi}^{\mathrm{r}},k) = \left|\sum_{l=0}^{L_{\mathrm{r}}-1}|g_l^{\mathrm{r}}(\phi^{\mathrm{r}})|\mathrm{e}^{-\jmath(\psi_l^{\mathrm{r}}-\alpha_l^{\mathrm{r}}kT)}\right|^2 \quad (19)$$
$$= \sum_{l=0}^{L_{\mathrm{r}}-1}|g_l^{\mathrm{r}}(\phi^{\mathrm{r}})|^2 + 2\sum_{l=0}^{L_{\mathrm{r}}-2}\sum_{i=l+1}^{L_{\mathrm{r}}-1}|g_l^{\mathrm{r}}(\phi^{\mathrm{r}})||g_i^{\mathrm{r}}(\phi^{\mathrm{r}})| \times \cos\left(\psi_i^{\mathrm{r}} - \psi_l^{\mathrm{r}} - (\alpha_i^{\mathrm{r}} - \alpha_l^{\mathrm{r}})kT\right). \quad (20)$$

and

$$G_{\mathrm{s}}(\phi^{\mathrm{s}},\boldsymbol{\alpha}^{\mathrm{s}},\boldsymbol{\psi}^{\mathrm{s}},k) = \left|\sum_{m=0}^{L_{\mathrm{s}}-1}|g_m^{\mathrm{s}}(\phi^{\mathrm{s}})|\mathrm{e}^{-\jmath(\psi_l^{\mathrm{s}}-\alpha_l^{\mathrm{s}}kT)}\right|^2. \quad (21)$$

From Section II-D, we know that P_{r} is assumed approximately constant over burst duration. Thus, we normalize the SNR with respect to $P_{\mathrm{r}}/\sigma_{\mathrm{n}}^2$ and we sum over a burst of K consecutive packets to obtain the normalized sum-SNR given by

$$S_{\mathrm{a}}(\phi^{\mathrm{r}},\phi^{\mathrm{s}},\boldsymbol{\alpha}^{\mathrm{r}},\boldsymbol{\alpha}^{\mathrm{s}},\boldsymbol{\psi}^{\mathrm{r}},\boldsymbol{\psi}^{\mathrm{s}}) = \sigma_{\mathrm{n}}^2/P_{\mathrm{r}}\sum_{k=0}^{K-1}\gamma_k^{(\mathrm{a})}$$
$$= K\overline{G}(\phi^{\mathrm{r}},\phi^{\mathrm{s}}) + J_{\mathrm{a}}(\phi^{\mathrm{r}},\phi^{\mathrm{s}},\boldsymbol{\alpha}^{\mathrm{r}},\boldsymbol{\alpha}^{\mathrm{s}},\boldsymbol{\psi}^{\mathrm{r}},\boldsymbol{\psi}^{\mathrm{s}}). \quad (22)$$

That is, the sum-SNR $S_{\mathrm{a}}(.)$ has a part that depends only on the AOA and AOD,

$$\overline{G}(\phi^{\mathrm{r}},\phi^{\mathrm{s}}) = \sum_{l=0}^{L_{\mathrm{r}}-1}\frac{|g_l^{\mathrm{r}}(\phi^{\mathrm{r}})|^2}{L_{\mathrm{r}}}\sum_{m=0}^{L_{\mathrm{s}}-1}\frac{|g_m^{\mathrm{s}}(\phi^{\mathrm{s}})|^2}{L_{\mathrm{s}}}, \quad (23)$$

and a part that captures the channel variation $J_{\mathrm{a}}(\cdot)$, which, with some simplification of notation, and introduction of the operator

$$\Delta x_{l,i} \triangleq x_i - x_l, \quad (24)$$

can be expressed according to (25)–(26) on top of the page.

[2]Consideration of interference is important, but it is outside the scope of this work and left for future work, as discussed further in Section VI.

2) Optimization Problem: We are interested in finding the design parameters $\boldsymbol{\alpha}^{\mathrm{r}}, \boldsymbol{\alpha}^{\mathrm{s}}$ that yield a robust system, i.e., that maximize the sum-SNR for worst-case AOA, AOD. Besides that, we need to account for the worst-case effective channel phases $(\boldsymbol{\psi}^{\mathrm{r}}, \boldsymbol{\psi}^{\mathrm{s}})$, which depend on the initial unknown offset of phase shifters $(\beta_l^{\mathrm{r}}, \beta_m^{\mathrm{s}})$ at both Rx and Tx. Thus, the problem can be stated formally as

$$(\tilde{\boldsymbol{\alpha}}^{\mathrm{r}}, \tilde{\boldsymbol{\alpha}}^{\mathrm{s}}) = \arg \sup_{(\boldsymbol{\alpha}^{\mathrm{r}}, \boldsymbol{\alpha}^{\mathrm{s}})} \inf_{\substack{(\phi^{\mathrm{r}}, \phi^{\mathrm{s}}) \\ (\boldsymbol{\psi}^{\mathrm{r}}, \boldsymbol{\psi}^{\mathrm{s}})}} S_{\mathrm{a}}(\phi^{\mathrm{r}}, \phi^{\mathrm{s}}, \boldsymbol{\alpha}^{\mathrm{r}}, \boldsymbol{\alpha}^{\mathrm{s}}, \boldsymbol{\psi}^{\mathrm{r}}, \boldsymbol{\psi}^{\mathrm{s}}), \tag{27}$$

where, $\boldsymbol{\alpha}^{\mathrm{r}} \in \mathbb{R}^{L_{\mathrm{r}}}$, $\boldsymbol{\alpha}^{\mathrm{s}} \in \mathbb{R}^{L_{\mathrm{s}}}$, $\boldsymbol{\psi}^{\mathrm{r}} \in [0, 2\pi)^{L_{\mathrm{r}}}$, $\boldsymbol{\psi}^{\mathrm{s}} \in [0, 2\pi)^{L_{\mathrm{s}}}$ and $\phi^{\mathrm{r}}, \phi^{\mathrm{s}} \in [0, 2\pi)$. The solutions to this problem can be deduced from the following theorem.

Theorem 1. *Given S_{a} defined in* (22) *and $L_{\mathrm{r}} + L_{\mathrm{s}} > 2$, let*

$$S_{\mathrm{a}}^{\star}(\phi^{\mathrm{r}}, \phi^{\mathrm{s}}) \triangleq \sup_{(\boldsymbol{\alpha}^{\mathrm{r}}, \boldsymbol{\alpha}^{\mathrm{s}})} \inf_{(\boldsymbol{\psi}^{\mathrm{r}}, \boldsymbol{\psi}^{\mathrm{s}})} S_{\mathrm{a}}(\phi^{\mathrm{r}}, \phi^{\mathrm{s}}, \boldsymbol{\alpha}^{\mathrm{r}}, \boldsymbol{\alpha}^{\mathrm{s}}, \boldsymbol{\psi}^{\mathrm{r}}, \boldsymbol{\psi}^{\mathrm{s}}).$$

Then, for any AOA, AOD, we have

(i) The objective function is upper bounded as

$$S_{\mathrm{a}}^{\star}(\phi^{\mathrm{r}}, \phi^{\mathrm{s}}) \leq K \overline{G}(\phi^{\mathrm{r}}, \phi^{\mathrm{s}}). \tag{28}$$

(ii) If $L_{\mathrm{r}} L_{\mathrm{s}} \leq K$, the upper bound is achievable

$$S_{\mathrm{a}}^{\star}(\phi^{\mathrm{r}}, \phi^{\mathrm{s}}) = K \overline{G}(\phi^{\mathrm{r}}, \phi^{\mathrm{s}}). \tag{29}$$

(iii) A solution $(\tilde{\boldsymbol{\alpha}}^{\mathrm{r}}, \tilde{\boldsymbol{\alpha}}^{\mathrm{s}})$ yields (29)*, when $L_{\mathrm{r}} L_{\mathrm{s}} \leq K$ if*

$$\Delta\tilde{\alpha}_{l,i}^{\mathrm{r}} T/2 \in \mathcal{X}^*, \tag{30a}$$

$$\Delta\tilde{\alpha}_{m,j}^{\mathrm{s}} T/2 \in \mathcal{X}^*, \tag{30b}$$

$$(\Delta\tilde{\alpha}_{l,i}^{\mathrm{r}} \pm \Delta\tilde{\alpha}_{m,j}^{\mathrm{s}}) T/2 \in \mathcal{X}^*, \tag{30c}$$

where $\mathcal{X}^* = \{q\pi/K : q \in \mathbb{Z}\} \setminus \{n\pi : n \in \mathbb{Z}\}$, $0 \leq l < i \leq L_{\mathrm{r}} - 1$ and $0 \leq m < j \leq L_{\mathrm{s}} - 1$. The condition is restricted to (30b) *or* (30a)*, when $L_{\mathrm{r}} = 1$ or $L_{\mathrm{s}} = 1$, respectively.*

(iv) If $|g_l^{\mathrm{r}}(\phi^{\mathrm{r}})| > 0$, $\forall l$ and $|g_m^{\mathrm{s}}(\phi^{\mathrm{s}})| > 0$, $\forall m$, then (29) $\implies$ (30) *and $L_{\mathrm{r}} L_{\mathrm{s}} \leq K$.*

Proof. See Appendix A. □

Remark 1. *The solutions satisfying* (30) *are independent of ϕ^{r} and ϕ^{s}, and thus they solve* (27) *when $L_{\mathrm{r}} L_{\mathrm{s}} \leq K$.*

Remark 2. *An optimal solution $(\tilde{\boldsymbol{\alpha}}^{\mathrm{r}}, \tilde{\boldsymbol{\alpha}}^{\mathrm{s}})$ (i.e., satisfies* (30)*) achieve for $\boldsymbol{\psi}^{\mathrm{r}} \in [0, 2\pi)^{L_{\mathrm{r}}}$, $\boldsymbol{\psi}^{\mathrm{s}} \in [0, 2\pi)^{L_{\mathrm{s}}}$,*

$$S_{\mathrm{a}}(\phi^{\mathrm{r}}, \phi^{\mathrm{s}}, \tilde{\boldsymbol{\alpha}}^{\mathrm{r}}, \tilde{\boldsymbol{\alpha}}^{\mathrm{s}}, \boldsymbol{\psi}^{\mathrm{r}}, \boldsymbol{\psi}^{\mathrm{s}}) = K \overline{G}(\phi^{\mathrm{r}}, \phi^{\mathrm{s}}). \tag{31}$$

Proof. See Appendix A. □

Theorem 1 indicates that choosing a set of phase slopes satisfying (30) maximizes the sum-SNR for the worst-case effective channel phase vectors, for all AOA, AOD including the worst-case directions. Thus, the solutions satisfying (30) are solutions to (27), when $L_{\mathrm{r}} L_{\mathrm{s}} \leq K$. Assuming an antenna system with $|g_l^{\mathrm{r}}(\phi^{\mathrm{r}})| > 0$, $\forall l$ and $|g_m^{\mathrm{s}}(\phi^{\mathrm{s}})| > 0$, $\forall m$, then we know that the only way to solve (27) is to use a set of phase slopes satisfying (30). That implies that (30) is a sufficient and necessary optimality condition in this case. Note that the last assumption on the antenna system is easily satisfied for physical antennas which typically radiate in all directions including nulls. These usually correspond to very low, but non-zero gains (several dBs below zero). Recalling (22), we see that Remark 2 points out that the optimal phase slopes average out the variation of sum-SNR due to effective channel phases, i.e., $J_{\mathrm{a}}(\phi^{\mathrm{r}}, \phi^{\mathrm{s}}, \tilde{\boldsymbol{\alpha}}^{\mathrm{r}}, \tilde{\boldsymbol{\alpha}}^{\mathrm{s}}, \boldsymbol{\psi}^{\mathrm{r}}, \boldsymbol{\psi}^{\mathrm{s}}) = 0$, $\forall(\boldsymbol{\psi}^{\mathrm{r}}, \boldsymbol{\psi}^{\mathrm{s}})$. Since the optimal sum-SNR is proportional to $\overline{G}(\phi^{\mathrm{r}}, \phi^{\mathrm{s}})$, we refer to $\overline{G}$ as the effective radiation pattern realized using ABN.

The theorem results are general, and they apply to the special cases $L_{\mathrm{s}} = 1$ or $L_{\mathrm{r}} = 1$. The optimality conditions boil down to $L_{\mathrm{r}} \leq K$ and (30a) for the former special case, and to $L_{\mathrm{s}} \leq K$ and (30b) for the latter. The system with $L_{\mathrm{s}} = 1$ has already been studied in [4]. The derived condition (30a) coincides with the optimality condition of phase slopes obtained in [4, Theorem 1, eq. (18)]. However, in that work, it was shown that the phase slopes satisfying (30a) ensure a lower bound on the objective function when $L_{\mathrm{r}} \leq K$, while their optimality was shown to hold only in the special cases of $L_{\mathrm{r}} \in \{2, 3\}$. Here, Theorem 1 extends the optimality of phase slopes satisfying (30a) to any system with $L_{\mathrm{r}} \leq K$ ($L_{\mathrm{s}} = 1$).

Given the conditions (30) and $L_{\mathrm{r}} L_{\mathrm{s}} \leq K$ we can derive phase slopes constructions that achieve optimality. These are stated in the following corollary.

Corollary 1. *If $L_{\mathrm{r}} L_{\mathrm{s}} \leq K$, then the following phase slopes*

$$\tilde{\alpha}_l^{\mathrm{r}} = l \frac{2\pi}{KT}, \ \tilde{\alpha}_m^{\mathrm{s}} = m L_{\mathrm{r}} \frac{2\pi}{KT}, \tag{32}$$

$$\tilde{\alpha}_l^{\mathrm{r}} = l L_{\mathrm{s}} \frac{2\pi}{KT}, \ \tilde{\alpha}_m^{\mathrm{s}} = m \frac{2\pi}{KT}, \tag{33}$$

where $0 \leq l \leq L_{\mathrm{r}} - 1$ and $0 \leq m \leq L_{\mathrm{s}} - 1$, satisfy (30) *and thus are optimal.*

Proof. See Appendix A (Lemma 6). □

These two phase slopes constructions are not unique. The construction (32) yields the same receiver phase slopes that were suggested in [4, Theorem 1, eq. (19)]. These constructions require the knowledge of the number of antennas at the receiver or the transmitter. So far, we assumed that all receiving VUs have the same number of antennas. However, we can generalize this solution to VUs with different numbers of antennas.

3) Supporting VUs with Different Number of Antennas: Instead of assuming that all users have the same number of antennas, let us assume that the maximum number of antennas any user can have is $L_{\mathrm{r,max}}$ at the receiver and $L_{\mathrm{s,max}}$ at the transmitter. Moreover, we assume that all users are aware of these two parameters, and they satisfy $L_{\mathrm{s,max}} L_{\mathrm{r,max}} \leq K$. Following that we can use (30) and attempt to find phase slopes that work for any $L_{\mathrm{s}} \leq L_{\mathrm{s,max}}$ and $L_{\mathrm{r}} \leq L_{\mathrm{r,max}}$. The following corollary gives us such a solution.

Corollary 2. *The phase slopes constructions given by*

$$\tilde{\alpha}_l^{\mathrm{r}} = l \frac{2\pi}{KT}, \quad \tilde{\alpha}_m^{\mathrm{s}} = m L_{\mathrm{r,max}} \frac{2\pi}{KT}, \tag{34}$$

$$\tilde{\alpha}_l^{\mathrm{r}} = l L_{\mathrm{s,max}} \frac{2\pi}{KT}, \quad \tilde{\alpha}_m^{\mathrm{s}} = m \frac{2\pi}{KT}, \tag{35}$$

where $0 \leq l \leq L_{\mathrm{r}}-1$, $0 \leq m \leq L_{\mathrm{s}}-1$ *satisfy* (30) *when* $L_{\mathrm{r,max}}L_{\mathrm{s,max}} \leq K$, *and* $L_{\mathrm{r}} \leq L_{\mathrm{r,max}}$, $L_{\mathrm{s}} \leq L_{\mathrm{s,max}}$.

Proof. This can be reached straightforwardly by substituting in (30) and using the fact that $L_{\mathrm{r,max}}L_{\mathrm{s,max}} \leq K$. (For exact details see the proof of Corollary 1.) □

Note that in such a case, a transmitter does not need to know the number of antennas at the receiver. However, knowledge of the maximum number of antennas that a user can have is required.

The phase slopes at the Tx do not depend on the AOA, AOD, nor on the far field functions of antennas. This implies that a transmitter can use an ABN beamforming vector with fixed phase slopes to achieve optimal performance for any VU including the worst one (i.e., including the user with the worst sum-SNR). Hence, the solutions to (27) solve the problem of maximizing the sum-SNR for the worst receiving user, also when VUs have different numbers of antennas $L_{\mathrm{r}} \leq L_{\mathrm{r,max}}$ and different far field functions.

B. Design of the Transmit Antenna Switching Network

1) Deriving the SNR per Packet: We follow the same steps as done when deriving the SNR for the ABN scheme. Given the received signal (8) with effective channel gain $c^{(\mathrm{b})}$ (12), and adopting the assumptions in Section II-D, the SNR for the k^{th} packet, $k = 0, 1, \cdots, K-1$ can be expressed as

$$\gamma_k^{(\mathrm{b})} = \frac{P_{\mathrm{r}}}{L_{\mathrm{r}}\sigma_{\mathrm{n}}^2}|c^{(\mathrm{b})}(kT)|^2 = \frac{P_{\mathrm{r}}}{\sigma_{\mathrm{n}}^2}|g_m^{\mathrm{s}}(\phi^{\mathrm{s}})|^2\frac{G_{\mathrm{r}}(\phi^{\mathrm{r}},\boldsymbol{\alpha}^{\mathrm{r}},\boldsymbol{\psi}^{\mathrm{r}},k)}{L_{\mathrm{r}}}, \tag{36}$$

where $m = \mathrm{mod}(k, L_{\mathrm{s}})$, $G_{\mathrm{r}}(.)$ is given by (19), and $\boldsymbol{\psi}^{\mathrm{r}}$ is an L_{r}-vector with elements ψ_l^{r} defined in (16). ASN switches antenna after each transmission. To simplify its analysis, we assume that $K/L_{\mathrm{s}} = K_{\mathrm{r}}$ is an integer, implying that each antenna element is used to transmit an equal number of K_{r} packets within a burst of K packets. Then, the ASN normalized sum-SNR is given by

$$S_{\mathrm{b}}(\phi^{\mathrm{r}},\phi^{\mathrm{s}},\boldsymbol{\alpha}^{\mathrm{r}},\boldsymbol{\psi}^{\mathrm{r}}) = \sigma_{\mathrm{n}}^2/P_{\mathrm{r}}\sum_{k=0}^{K-1}\gamma_k^{(\mathrm{b})} \tag{37}$$

$$= \sum_{m=0}^{L_{\mathrm{s}}-1}|g_m^{\mathrm{s}}(\phi^{\mathrm{s}})|^2\sum_{k'=0}^{K_{\mathrm{r}}-1}\frac{G_{\mathrm{r}}(\phi^{\mathrm{r}},\boldsymbol{\alpha}^{\mathrm{r}},\boldsymbol{\psi}^{\mathrm{r}},m+k'L_{\mathrm{s}})}{L_{\mathrm{r}}}. \tag{38}$$

From the expression, we observe that a packet is sent using the m^{th} antenna periodically every L_{s} transmissions. Using (20), the normalized sum-SNR can be elaborated and stated as

$$S_{\mathrm{b}}(\phi^{\mathrm{r}},\phi^{\mathrm{s}},\boldsymbol{\alpha}^{\mathrm{r}},\boldsymbol{\psi}^{\mathrm{r}}) = K\overline{G}(\phi^{\mathrm{r}},\phi^{\mathrm{s}}) + J_{\mathrm{b}}(\phi^{\mathrm{r}},\phi^{\mathrm{s}},\boldsymbol{\alpha}^{\mathrm{r}},\boldsymbol{\psi}^{\mathrm{r}}), \tag{39}$$

where $\overline{G}(\phi^{\mathrm{r}},\phi^{\mathrm{s}})$ is given by (23) and

$$J_{\mathrm{b}}(\phi^{\mathrm{r}},\phi^{\mathrm{s}},\boldsymbol{\alpha}^{\mathrm{r}},\boldsymbol{\psi}^{\mathrm{r}}) = \sum_{m=0}^{L_{\mathrm{s}}-1}|g_m^{\mathrm{s}}(\phi^{\mathrm{s}})|^2\sum_{l=0}^{L_{\mathrm{r}}-2}\sum_{i=l+1}^{L_{\mathrm{r}}-1}c'_{l,i}(\phi^{\mathrm{r}})$$
$$\times\sum_{k'=0}^{K_{\mathrm{r}}-1}\cos\left(\Delta\psi_{l,i}^{\mathrm{r}} - \Delta\alpha_{l,i}^{\mathrm{r}}(m+k'L_{\mathrm{s}})T\right), \tag{40}$$

where $c'_{l,i}(\phi^{\mathrm{r}})$ is defined in (26).

2) Optimization: For the ASN only the receiver phase slopes are to be found. The optimization problem has a similar form to (27), and it is given by

$$\tilde{\boldsymbol{\alpha}}^{\mathrm{r}} = \arg\sup_{\boldsymbol{\alpha}^{\mathrm{r}}\in\mathbb{R}^{L_{\mathrm{r}}}}\inf_{\substack{(\phi^{\mathrm{s}},\phi^{\mathrm{r}})\\ \boldsymbol{\psi}^{\mathrm{r}}\in[0,2\pi)^{L_{\mathrm{r}}}}} S_{\mathrm{b}}(\phi^{\mathrm{r}},\phi^{\mathrm{s}},\boldsymbol{\alpha}^{\mathrm{r}},\boldsymbol{\psi}^{\mathrm{r}}). \tag{41}$$

Note that ASN inherently treats all receiving VUs the same. Thus, in spite of how many antennas and the type of far field functions different receiving VUs have, the optimization problem (41) and its solutions apply to any user including the one experiencing the worst sum-SNR. The solution to the problem can be deduced from the following theorem.

Theorem 2. *Let* S_{b} *be as defined in* (39)*,* $K/L_{\mathrm{s}} = K_{\mathrm{r}} \in \mathbb{Z}$*,* $L_{\mathrm{r}} > 1$*, and let*

$$S_{\mathrm{b}}^{\star}(\phi^{\mathrm{r}},\phi^{\mathrm{s}}) \triangleq \sup_{\boldsymbol{\alpha}^{\mathrm{r}}}\inf_{\boldsymbol{\psi}^{\mathrm{r}}} S_{\mathrm{b}}(\phi^{\mathrm{r}},\phi^{\mathrm{s}},\boldsymbol{\alpha}^{\mathrm{r}},\boldsymbol{\psi}^{\mathrm{r}}). \tag{42}$$

Then, for any $(\phi^{\mathrm{r}},\phi^{\mathrm{s}})$

(i) The function is bounded as

$$S_{\mathrm{b}}^{\star}(\phi^{\mathrm{r}},\phi^{\mathrm{s}}) \leq K\overline{G}(\phi^{\mathrm{r}},\phi^{\mathrm{s}}). \tag{43}$$

(ii) If $L_{\mathrm{r}} \leq K_{\mathrm{r}}$ *the bound is achievable, i.e.,*

$$S_{\mathrm{b}}^{\star}(\phi^{\mathrm{r}},\phi^{\mathrm{s}}) = K\overline{G}(\phi^{\mathrm{r}},\phi^{\mathrm{s}}), \tag{44}$$

with solutions that satisfy

$$L_{\mathrm{s}}\Delta\tilde{\alpha}_{l,i}^{\mathrm{r}}T/2 \in \mathcal{X}_{K_{\mathrm{r}}}^{*}, \tag{45}$$

where $\mathcal{X}_{K_{\mathrm{r}}}^{*} = \{q\pi/K_{\mathrm{r}} : q \in \mathbb{Z}\} \setminus \{n\pi : n \in \mathbb{Z}\}$*, and* $0 \leq l < i \leq L_{\mathrm{r}}-1$.

(iii) Assuming $|g_l^{\mathrm{r}}(\phi^{\mathrm{r}})| > 0$, $\forall l$, $|g_m^{\mathrm{s}}(\phi^{\mathrm{s}})| > 0$, $\forall m$, *and* $|g_m^{\mathrm{s}}(\phi^{\mathrm{s}})| \neq C$, $\forall m$, *then* (44) $\implies$ (45) *and* $L_{\mathrm{r}} \leq K_{\mathrm{r}}$.

(iv) One optimal solution is given by

$$\tilde{\alpha}_l^{\mathrm{r}} = l\frac{2\pi}{KT}, \quad l = 0, 1, \cdots L_{\mathrm{r}}-1,\ L_{\mathrm{r}} \leq K_{\mathrm{r}}. \tag{46}$$

Proof. See Appendix B. □

Similarly to the ABN case, the solutions satisfying (45) are independent of the signal directions $(\phi^{\mathrm{r}},\phi^{\mathrm{s}})$, hence they solve (41) when $L_{\mathrm{r}} \leq K_{\mathrm{r}} = K/L_{\mathrm{s}}$. Moreover, under the assumptions indicated in Theorem 2 *(iii)*, (45) is a sufficient and necessary optimality condition for (41). Note that, $|g_m^{\mathrm{s}}(\phi^{\mathrm{s}})| = C$, $\forall m$, is a special case where the antenna system is equivalent to $1 \times L_{\mathrm{r}}$ system, and thus it is covered by Theorem 1. In particular, for $|g_m^{\mathrm{s}}(\phi^{\mathrm{s}})| = C > 0$, $\forall m$, and $|g_l^{\mathrm{r}}(\phi^{\mathrm{r}})| > 0$, $\forall l$, (44) $\implies$ (30a) and $L_{\mathrm{r}} \leq K$. We observe that the optimality condition related to the number of antennas $L_{\mathrm{r}} \leq K_{\mathrm{r}} = K/L_{\mathrm{s}}$ is equivalent to what has been obtained for the ABN scheme ($L_{\mathrm{r}}L_{\mathrm{s}} \leq K$). The phase slopes optimality condition (45) is, on the other hand, simpler than (30).

We can draw two main conclusions from the theorem. First, the performance achieved using an ASN is identical to that of an ABN, $S_{\mathrm{b}}^{\star}(\phi^{\mathrm{r}},\phi^{\mathrm{s}}) = S_{\mathrm{a}}^{\star}(\phi^{\mathrm{r}},\phi^{\mathrm{s}})$. Hence, the main difference between the two is the implementation. Second, the suggested optimal phase slopes construction (46) at the receiver side when an ASN is used, coincides with the phase slopes construction (32) (or (34)), which is used to combine the antenna signals when an ABN is used at the transmitter. Hence, we

can design the receiver ACN such that it optimally combines signals arriving from both ABN and ASN transmitters. Such a receiver does not require any knowledge of the number of antennas used at the transmitter side.

An important aspect of Theorem 2 is the assumption $K_{\mathrm{r}} = K/L_{\mathrm{s}} \in \mathbb{Z}$, which can be easily met if all VUs use the same number of transmit antennas, however, in a context where VUs are equipped with different numbers of transmit antennas it may not be easily met. In the following, we investigate the implications of the assumption in such context.

3) VUs with Different Number of Transmit Antennas: Assume that the maximum number of antennas that can be used by any VU to transmit and receive are $L_{\mathrm{s,max}}$ and $L_{\mathrm{r,max}}$, respectively. Further, assume that $K/L_{\mathrm{s,max}} \in \mathbb{Z}$, and $L_{\mathrm{r,max}} \leq K/L_{\mathrm{s,max}}$. Receiving VUs employ a phase slope vector $\tilde{\boldsymbol{\alpha}}^{\mathrm{r}}$ that satisfies (46). This selection of phase slopes is optimal for any Tx with L_{s} satisfying $K/L_{\mathrm{s}} \in \mathbb{Z}$ (including $L_{\mathrm{s}} = L_{\mathrm{s,max}}$). The optimal sum-SNR is given by (44). For transmitting VUs with $K/L_{\mathrm{s}} \notin \mathbb{Z}$, the phase slopes are not known to achieve the optimal sum-SNR. The performance is governed in this case by

$$\inf_{\boldsymbol{\psi}^{\mathrm{r}} \in [0,2\pi)^{L_{\mathrm{r}}}} S_{\mathrm{b}}(\phi^{\mathrm{r}}, \phi^{\mathrm{s}}, \tilde{\boldsymbol{\alpha}}^{\mathrm{r}}, \boldsymbol{\psi}^{\mathrm{r}}), \tag{47}$$

where S_{b} is as defined in (37) (Note that (38)–(40) hold when $K/L_{\mathrm{s}} \in \mathbb{Z}$). No analytical solution to (47) is available. However, a numerical characterization of the expression and a comparison with the optimal sum-SNR attained by ABN will be shown in the numerical results section.

C. ABN and ASN Transceivers

In spite of the advantage of ABN over ASN in supporting transmission with different numbers of antennas, we have shown that the two structures yield the same performance in the general case. However, each structure puts different requirements on the transceiver. In particular, an ABN-ACN transceiver needs to support two different sets of phase shifter slopes, one tuned for transmission ($\{\tilde{\alpha}^{\mathrm{s}}_m\}$) and another for reception ($\{\tilde{\alpha}^{\mathrm{r}}_l\}$). On the other hand, an ASN-ACN transceiver has to support one set of phase shifter slopes ($\{\tilde{\alpha}^{\mathrm{r}}_l\}$), and be capable of transmitting with L_{s} times higher power than the power transmitted on each antenna branch using ABN. From these requirements stem the main implementation trade-offs between the two structures, and depending on how transceivers with such requirements are implemented, ABN and ASN may differ in cost and complexity.

D. Alamouti Scheme Performance

In the following, we compare the performance of the developed analog multiple antenna system with the performance of the fully digital Alamouti scheme. The scheme does not rely on CSI, and therefore it is suitable for the broadcast scenario we are considering. Assume that the receiver uses an ACN, while the transmitter with $L_{\mathrm{s}} = 2$ applies an Alamouti encoding in space-time domain, in accordance with an orthogonal frequency division multiplexing (OFDM) signal (see e.g., [20], [21, Ch. 22])[3]. Assume that packets are composed of N_{sym} OFDM symbols, $\boldsymbol{s}_i$, each composed of N subcarriers. The Alamouti encoding matrix is given by,

$$\begin{bmatrix} \boldsymbol{s}_0 & \boldsymbol{s}_1 \\ -\boldsymbol{s}_1^* & \boldsymbol{s}_0^* \end{bmatrix} \begin{matrix} \rightarrow \\ \downarrow \end{matrix} \begin{matrix} \text{space} \\ \text{time} \end{matrix} \tag{48}$$

where $\boldsymbol{s}_0$ and $\boldsymbol{s}_1$ are two consecutive OFDM symbols. After applying the space-time mapping, symbols are converted to time domain, appended a cyclic prefix, then sent over the channel. Given the channel gain $h_{l,m}$ as defined in (1), let $\boldsymbol{H}_m = [h_{0,m}, h_{1,m}, \cdots, h_{L_{\mathrm{r}}-1,m}]^{\mathsf{T}}/a(t)$ denotes the m^{th} column of $\boldsymbol{H}$, where $a(t) = |a(t)|\mathrm{e}^{-\jmath 2\pi f_{\mathrm{c}} \tau_0(t)}$, then the received signal after ACN combining with $\boldsymbol{w}$ as defined in (6), can be modeled as

$$r(t) = \frac{1}{\sqrt{2}} a(t) \boldsymbol{w}^{\mathsf{H}} (\bar{x}_0(t) \boldsymbol{H}_0 + \bar{x}_1(t) \boldsymbol{H}_1) + \boldsymbol{w}^{\mathsf{H}} \boldsymbol{n}, \tag{49}$$

where $\bar{x}_0(t)$ and $\bar{x}_1(t)$ are the transmitted Alamouti encoded signals delayed by $\tau_0(t)$, and $\boldsymbol{w}^{\mathsf{H}}\boldsymbol{n}$ is a zero-mean white Gaussian noise with variance $\mathbb{E}\{|\boldsymbol{w}^{\mathsf{H}}\boldsymbol{n}|^2\} = L_{\mathrm{r}}\sigma_{\mathrm{n}}^2$.

Given the assumptions in Section II-D, we can approximate $\bar{c}_m = \boldsymbol{w}^{\mathsf{H}} \boldsymbol{H}_m/\sqrt{2}$, $m \in \{0, 1\}$, for the k^{th} packet, as

$$\frac{1}{\sqrt{2}} g^{\mathrm{s}}_m(\phi^{\mathrm{s}}) \mathrm{e}^{\jmath \Omega^{\mathrm{s}}_m} \sum_{l=0}^{L_{\mathrm{r}}-1} |g^{\mathrm{r}}_l(\phi^{\mathrm{r}})| \mathrm{e}^{-\jmath(\psi^{\mathrm{r}}_l - \alpha^{\mathrm{r}}_l kT)}, \tag{50}$$

where ψ^{r}_l is given by (16). To decode the message, the receiver uses two consecutive OFDM symbols (after discarding the cyclic prefix and conversion to the frequency domain), as follows

$$\boldsymbol{y}_0 = \bar{c}_0 \boldsymbol{D}_{\mathrm{a}} \boldsymbol{s}_0 + \bar{c}_1 \boldsymbol{D}_{\mathrm{a}} \boldsymbol{s}_1 + \boldsymbol{z}_0, \tag{51}$$

$$\boldsymbol{y}_1 = -\bar{c}_0 \boldsymbol{D}_{\mathrm{a}} \boldsymbol{s}_1^* + \bar{c}_1 \boldsymbol{D}_{\mathrm{a}} \boldsymbol{s}_0^* + \boldsymbol{z}_1, \tag{52}$$

where $\boldsymbol{D}_{\mathrm{a}} = \bar{\boldsymbol{D}}^{(i)}_{\mathrm{a}}$, is a diagonal matrix carrying the frequency response of the sampled finite channel impulse response associated with $a(t)$, at symbol duration i, and it is assumed constant over two consecutive OFDM symbols duration (follows from the basic assumption of Alamouti scheme [11]). The vectors $\boldsymbol{z}_0$, $\boldsymbol{z}_1$, are zero-mean independent white Gaussian noises with variance $\mathbb{E}\{|\boldsymbol{z}_i|^2\} = L_{\mathrm{r}}\sigma_{\mathrm{n}}^2/N_{\mathrm{sym}}$, $i = 1, 2$. Forming the two combined signals, $(\bar{c}_0^* \boldsymbol{D}_{\mathrm{a}}^* \boldsymbol{y}_0 + \bar{c}_1 \boldsymbol{D}_{\mathrm{a}} \boldsymbol{y}_1^*)$ and $(\bar{c}_1^* \boldsymbol{D}_{\mathrm{a}}^* \boldsymbol{y}_0 - \bar{c}_0 \boldsymbol{D}_{\mathrm{a}} \boldsymbol{y}_1^*)$, and employing (49) we can deduce the normalized SNR of the k^{th} packet

$$\frac{\sigma_{\mathrm{n}}^2}{P_{\mathrm{r}}} \gamma_k^{(\mathrm{Al})} = \frac{G_{\mathrm{r}}(\phi^{\mathrm{r}}, \boldsymbol{\alpha}^{\mathrm{r}}, \boldsymbol{\psi}^{\mathrm{r}}, k)}{L_{\mathrm{r}}} \sum_{m=0}^{L_{\mathrm{s}}-1} \frac{|g^{\mathrm{s}}_m(\phi^{\mathrm{s}})|^2}{L_{\mathrm{s}}}, \tag{53}$$

where $G_{\mathrm{r}}(\cdot)$ is given by (19). The average signal power is given in this case by $P_{\mathrm{r}} = \mathbb{E}\{|a(t)\bar{x}_0(t)|^2\} = \mathbb{E}\{|a(t)\bar{x}_1(t)|^2\} = \sum_{i=0}^{N_{\mathrm{sym}}-1} \mathbb{E}\{|\boldsymbol{D}_{\mathrm{a}} \boldsymbol{s}_i|^2\}$.

We can observe from (53) that optimizing the sum-SNR of the Alamouti scheme is equivalent to optimizing $\sum_{k=0}^{K-1} G_{\mathrm{r}}(\cdot)$ which is the sum-SNR of an ACN with L_{r} antennas. By

[3] Alamouti can be applied to OFDM in space-frequency domain as well (see e.g., [22]), and it is found to yield the same result.

Theorem 1 we can conclude that if $L_{\rm r} \leq K$ and phase slopes are chosen to satisfy (30a), we can achieve

$$\frac{\sigma_{\rm n}^2}{P_{\rm r}} \sum_{k=0}^{K-1} \gamma_k^{(\rm Al)} = S_{\rm a}^{\star}(\phi^{\rm r}, \phi^{\rm s}) = S_{\rm b}^{\star}(\phi^{\rm r}, \phi^{\rm s}). \tag{54}$$

Hence, in this scenario where the channel is modeled as a slowly varying dominant path, implying that the only available spatial diversity of the channel is due to the different far field functions of antennas (the propagation environment has spatial diversity of order one), ABN and ASN achieve similar performance compared to an Alamouti scheme. We note that Alamouti requires two digital ports at the transmitter. Moreover, it is not a transparent scheme since additional processing is needed at the receiver to decode the message. Therefore, it has a higher cost and higher complexity than ABN and ASN. From another perspective, the result of this section shows that an ACN receiver communicates optimally not only with ABN and ASN but also with an Alamouti transmitter.

IV. MRC Enhancement

The overall performance for VUs can be improved by employing an MRC digital combining stage after the analog combining at the receiver. Therefore, in this section, we use a hybrid combiner at the receiver. We follow a sub-connected configuration as in [6]. Antennas are divided into subgroups of $L_{{\rm r},p}$ elements that are combined in the analog domain using an ACN then fed to a digital port. We would like to show that the solutions provided by Theorem 1 and Theorem 2 are still optimal. To that end, we model the signal at port p of a given VU after the ACN following (8) as

$$r_p(t) = a(t)x(t)c_p(kT) + n_p(t), \tag{55}$$

where $kT \leq t \leq kT + T_{\rm m}$, and the approximation $c_p(t) \approx c_p(kT)$ follows from the assumptions in Section II-D. Employing MRC with coefficients $c_p^*(kT)/L_{{\rm r},p}$ [23], and since the noise is uncorrelated between the ports, the overall SNR per packet can be expressed as

$$\gamma_k^{(\rm d)} = \sum_{p=0}^{P-1} \frac{P_{\rm r}}{L_{{\rm r},p}\sigma_{\rm n}^2} |c_p(kT)|^2. \tag{56}$$

Given that we are using an ABN, the effective channel gain for the $k^{\rm th}$ packet is modeled by (14), with the following change in notation adopted,

$$g_l^{\rm r} \to g_{l,p}^{\rm r},\ \psi_l^{\rm r} \to \psi_{l,p}^{\rm r},\ \alpha_l^{\rm r} \to \alpha_{l,p}^{\rm r},\ L_{\rm r} \to L_{{\rm r},p}, \tag{57}$$

where $g_{l,p}^{\rm r}$, $\alpha_{l,p}^{\rm r}$, $\psi_{l,p}^{\rm r}$ are, respectively, the far field function, phase slope, and effective channel phase associated with the $l^{\rm th}$ receive antenna connected to port p. The effective channel gain can be explicitly expressed as

$$c_p^{(\rm a)}(kT) = \frac{1}{\sqrt{L_{\rm s}}} \sum_{m=0}^{L_{\rm s}-1} |g_m^{\rm s}(\phi^{\rm s})| {\rm e}^{-\jmath(\psi_m^{\rm s} - \alpha_m^{\rm s} kT)} \times \sum_{l=0}^{L_{{\rm r},p}-1} |g_{l,p}^{\rm r}(\phi^{\rm r})| {\rm e}^{-\jmath(\psi_{l,p}^{\rm r} - \alpha_{l,p}^{\rm r} kT)}. \tag{58}$$

Let $\boldsymbol{\psi}_p^{\rm r}$ and $\boldsymbol{\alpha}_p^{\rm r}$ be vectors with $L_{{\rm r},p}$ elements corresponding to $\psi_{l,p}^{\rm r}$ and $\alpha_{l,p}^{\rm r}$, respectively. Then, the normalized sum-SNR can be expressed as

$$\begin{aligned} S_{\rm d}(\phi^{\rm r}, \phi^{\rm s}, \boldsymbol{\alpha}^{\rm r}, \boldsymbol{\alpha}^{\rm s}, \boldsymbol{\psi}^{\rm r}, \boldsymbol{\psi}^{\rm s}) &= \sigma_{\rm n}^2/P_{\rm r} \sum_{k=0}^{K-1} \gamma_k^{(\rm d)} \\ &= \sum_{p=0}^{P-1} \sum_{k=0}^{K-1} \frac{G_{{\rm r},p}(\phi^{\rm r}, \boldsymbol{\alpha}_p^{\rm r}, \boldsymbol{\psi}_p^{\rm r}, k)}{L_{{\rm r},p}} \frac{G_{\rm s}(\phi^{\rm s}, \boldsymbol{\alpha}^{\rm s}, \boldsymbol{\psi}^{\rm s}, k)}{L_{\rm s}} \\ &= \sum_{p=0}^{P-1} S_{{\rm a},p}(\phi^{\rm r}, \phi^{\rm s}, \boldsymbol{\alpha}_p^{\rm r}, \boldsymbol{\alpha}^{\rm s}, \boldsymbol{\psi}_p^{\rm r}, \boldsymbol{\psi}^{\rm s}), \end{aligned} \tag{59}$$

where $\boldsymbol{\alpha}^{\rm r} = [\boldsymbol{\alpha}_0^{\rm r}, \boldsymbol{\alpha}_1^{\rm r}, \cdots, \boldsymbol{\alpha}_{P-1}^{\rm r}]$, $\boldsymbol{\psi}^{\rm r} = [\boldsymbol{\psi}_0^{\rm r}, \boldsymbol{\psi}_1^{\rm r}, \cdots, \boldsymbol{\psi}_{P-1}^{\rm r}]$, and $G_{{\rm r},p}(\cdot)$ is defined following (19) with change of notation (57) incorporated. The term $S_{{\rm a},p}(\cdot)$ is the same as (22),

$$\begin{aligned} S_{{\rm a},p}(\phi^{\rm r}, \phi^{\rm s}, \boldsymbol{\alpha}_p^{\rm r}, \boldsymbol{\alpha}^{\rm s}, \boldsymbol{\psi}_p^{\rm r}, \boldsymbol{\psi}^{\rm s}) &= K\overline{G}_p(\phi^{\rm r}, \phi^{\rm s}) \\ &\quad + J_{{\rm a},p}(\phi^{\rm r}, \phi^{\rm s}, \boldsymbol{\alpha}_p^{\rm r}, \boldsymbol{\alpha}^{\rm s}, \boldsymbol{\psi}_p^{\rm r}, \boldsymbol{\psi}^{\rm s}), \end{aligned} \tag{60}$$

where $\overline{G}_p$ and $J_{{\rm a},p}$ are given by (23) and (25), respectively, with (57) adopted (a sub-index p is added to $c_{l,i}, c'_{l,i}, d_{m,j}, d'_{m,j}$ in (26)).

As done earlier in Section III, we assume that all receiving VUs have the same number of antennas, the same far field functions, and additionally, we assume that they have the same number of ports. That allows us to define the worst user in the system based on the worst-case AOA, AOD. Following that, Theorem 1 already give us the solutions for any $(\phi^{\rm r}, \phi^{\rm s})$ to the per-port subproblems

$$(\tilde{\boldsymbol{\alpha}}_p^{\rm r}, \tilde{\boldsymbol{\alpha}}^{\rm s}) = \arg \underbrace{\sup_{(\boldsymbol{\alpha}_p^{\rm r}, \boldsymbol{\alpha}^{\rm s})} \inf_{(\boldsymbol{\psi}_p^{\rm r}, \boldsymbol{\psi}^{\rm s})} S_{{\rm a},p}(\phi^{\rm r}, \phi^{\rm s}, \boldsymbol{\alpha}_p^{\rm r}, \boldsymbol{\alpha}^{\rm s}, \boldsymbol{\psi}_p^{\rm r}, \boldsymbol{\psi}^{\rm s})}_{\triangleq S_{{\rm a},p}^{\star}(\phi^{\rm r}, \phi^{\rm s})}, \tag{61}$$

where, $\boldsymbol{\alpha}_p^{\rm r} \in \mathbb{R}^{L_{{\rm r},p}}$, $\boldsymbol{\alpha}^{\rm s} \in \mathbb{R}^{L_{\rm s}}$, $\boldsymbol{\psi}_p^{\rm r} \in [0, 2\pi)^{L_{{\rm r},p}}$, $\boldsymbol{\psi}^{\rm s} \in [0, 2\pi)^{L_{\rm s}}$. The optimal sum-SNR per subgroup of antennas is given by

$$\begin{aligned} S_{{\rm a},p}^{\star}(\phi^{\rm r}, \phi^{\rm s}) &= K\overline{G}_p(\phi^{\rm r}, \phi^{\rm s}) \\ &= K \sum_{l=0}^{L_{{\rm r},p}-1} \frac{|g_{l,p}^{\rm r}(\phi^{\rm r})|^2}{L_{{\rm r},p}} \sum_{m=0}^{L_{\rm s}-1} \frac{|g_m^{\rm s}(\phi^{\rm s})|^2}{L_{\rm s}}. \end{aligned} \tag{62}$$

To deduce the optimum of the overall problem, we can make use of the following lemma.

Lemma 1. *Let $S_{\rm d}$ be given by* (59)*, then*

$$\underbrace{\sup_{(\boldsymbol{\alpha}^{\rm r}, \boldsymbol{\alpha}^{\rm s})} \inf_{(\boldsymbol{\psi}^{\rm r}, \boldsymbol{\psi}^{\rm s})} S_{\rm d}(\phi^{\rm r}, \phi^{\rm s}, \boldsymbol{\alpha}^{\rm r}, \boldsymbol{\alpha}^{\rm s}, \boldsymbol{\psi}^{\rm r}, \boldsymbol{\psi}^{\rm s})}_{\triangleq S_{\rm d}^{\star}(\phi^{\rm r}, \phi^{\rm s})} \leq K \sum_{p=0}^{P-1} \overline{G}_p(\phi^{\rm r}, \phi^{\rm s}). \tag{63}$$

where $\overline{G}_p(\phi^{\rm r}, \phi^{\rm s})$ is given by (62)*.*

Proof. See Appendix C. □

The right-hand side of (63) is equal to $\sum_{p=0}^{P-1} S_{{\rm a},p}^{\star}(\phi^{\rm r}, \phi^{\rm s})$, which means that the solutions to the subproblems do satisfy the bound, and therefore are optimal for the overall problem.

For that to hold, the optimality conditions $L_{\mathrm{r},p}L_{\mathrm{s}} \leq K$ and (30) have to be satisfied for all ports p. Given that we design the phase slopes according to a certain construction, e.g., (32), then we can start with choosing $\tilde{\boldsymbol{\alpha}}^{\mathrm{s}}$ and $\tilde{\boldsymbol{\alpha}}^{\mathrm{r}}_{p}$ corresponding to the largest $L_{\mathrm{r},p}$, then the remaining $\tilde{\boldsymbol{\alpha}}^{\mathrm{r}}_{p'}$, $p' \neq p$ can be cloned on the already designed phase slope vector, and all optimality conditions will be satisfied.

Similar to what has been found earlier, $\tilde{\boldsymbol{\alpha}}^{\mathrm{s}}$ is independent of the far field function of the antennas, and it can be designed according to the maximum number of antennas a VU can have $L_{\mathrm{r,max}}$. For users with more than one digital port, the condition on the maximum number of antennas is given by $L_{\mathrm{r},p} \leq L_{\mathrm{r,max}}$, $\forall p$. Therefore, a transmitter can use the same ABN beamforming vector to achieve optimal performance for any user (in spite of the number of antennas, ports, and far field functions employed), including the worst one.

Due to the limitation of space, we will not go through a detailed analysis of the ASN. However, we point out that since the optimization parameters are restricted to $\boldsymbol{\alpha}^{\mathrm{r}}_{p}$ and $\boldsymbol{\psi}^{\mathrm{r}}_{p}$—which are independent of one port to another—by solving the subproblems per port using Theorem 2, we already solve the overall problem and achieve the same optimal performance given by

$$S^{\star}_{\mathrm{d}}(\phi^{\mathrm{r}},\phi^{\mathrm{s}}) = \sum_{p=0}^{P-1} S^{\star}_{\mathrm{a},p}(\phi^{\mathrm{r}},\phi^{\mathrm{s}}) = K\sum_{p=0}^{P-1} \overline{G}_{p}(\phi^{\mathrm{r}},\phi^{\mathrm{s}}). \quad (64)$$

Note that for a system with $L_{\mathrm{r},p} = L_{\mathrm{r}}/P$, $\forall p$ we get,

$$S^{\star}_{\mathrm{d}}(\phi^{\mathrm{r}},\phi^{\mathrm{s}}) = PK\overline{G}(\phi^{\mathrm{r}},\phi^{\mathrm{s}}). \quad (65)$$

Hence, the digital processing stage yields $10\log_{10}(P)$ dB higher gain for any $(\phi^{\mathrm{r}},\phi^{\mathrm{s}})$ compared to $S^{\star}_{\mathrm{a}}(\phi^{\mathrm{r}},\phi^{\mathrm{s}})$.

V. Numerical Results

In this section, we visualize the performance of ABN/ASN based on some examples of antenna radiation patterns that are shown in Fig. 3. There is an ideal omnidirectional antenna $A0$, and a non-ideal, synthetic omnidirectional antenna $A1$. Furthermore, there is a sector antenna $A2$, which is a back-to-back patch antenna designed by Smarteq[4] for vehicular applications. Finally, there is a directional antenna $A3$ with characteristics that are modeled following an analytical radiation pattern given by [24, Eq. 4]. All antenna types have the same average power gain in the azimuth plane.

Since the optimal phase slopes of ABN were found to be the same for any VU, including the worst one, and since ASN strategy treats all users the same, we quantify the performance of the two schemes in this section, assuming one transmitting and one receiving, reference VUs. Performance is assessed according to the sum-SNR of a burst of K consecutive CAM packets, with a focus on the worst-case AOA, AOD, such that we can characterize the robustness of V2V cooperative communication against unfavorable angles.

[4]Smarteq Wireless AB is a Swedish industrial partner specialized in developing antenna solutions for vehicle industry among others.

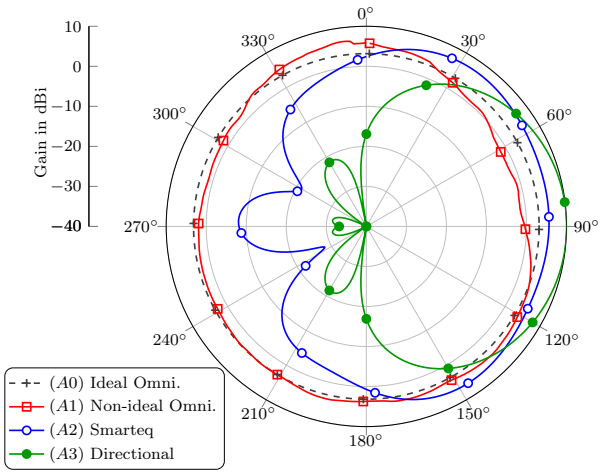

Fig. 3. Test antennas radiation patterns, $|g(\phi)|^2$, in dBi. All antennas have the same average power gain in the azimuth plane. (Omni. i.e., Omnidirectional).

A. Sum-SNR Achieved Using ABN/ASN

Consider the use of $A2$ sector antennas (Fig 3). Employing two $A2$ modules pointing 180 deg apart, we can enable full omnidirectional coverage. An ABN/ASN allows us to do that using a single transmit digital port. Note that, with a single digital port, and in absence of ABN/ASN, the use of one $A2$ module would yield very low performance in the direction where the antenna has low gain. Now, consider a communication link with $L_{\mathrm{s}} = 2$, $L_{\mathrm{r}} = 2$, and a burst of $K = 4 = L_{\mathrm{r}}L_{\mathrm{s}}$ consecutive CAM packets. Both the transmitter and the receiver are equipped with $A2$ antennas. We plot in Fig. 4 the CDF of the sum-SNR of 2×2 ABN/ASN-ACN system (with optimal phase slopes) for uniform AOA, AOD. We note that the sum-SNR is normalized with respect to $P_{\mathrm{r}}/\sigma^2_{\mathrm{n}}$, following (22) and (37), and that holds throughout this section. As indicated in Remark 2 the sum-SNR CDF is the same for any $\boldsymbol{\psi}^{\mathrm{r}} \in [0,2\pi)^{L_{\mathrm{r}}}, \boldsymbol{\psi}^{\mathrm{s}} \in [0,2\pi)^{L_{\mathrm{s}}}$, and it is identical for both ABN and ASN which coincides with our analytical result, $S^{\star}_{\mathrm{a}}(\phi^{\mathrm{r}},\phi^{\mathrm{s}}) = S^{\star}_{\mathrm{b}}(\phi^{\mathrm{r}},\phi^{\mathrm{s}})$. We recall that the optimal sum-SNR is proportional to the equivalent radiation pattern $\overline{G}(\phi^{\mathrm{r}},\phi^{\mathrm{s}})$, defined in (23). To observe how this is characterized at the transmitter side we visualize in Fig. 5 the term $\sum_{m=0}^{L_{\mathrm{s}}-1}|g^{\mathrm{s}}_{m}(\phi^{\mathrm{s}})|^2/L_{\mathrm{s}}$, which can be seen as the transmitter side equivalent pattern. We see that it has a nearly ideal omnidirectional coverage. The receiver equivalent pattern $\sum_{l=0}^{L_{\mathrm{r}}-1}|g^{\mathrm{r}}_{l}(\phi^{\mathrm{r}})|^2/L_{\mathrm{r}}$, which is omitted from the figure, has the same characteristics. From this example, we see that ABN/ASN yields an equivalent radiation pattern with improved omnidirectional characteristics (that implies improved robustness against unfavorable AOA, AOD).

We mentioned earlier that due to distortions caused by many factors including vehicle body, a practical omnidirectional pattern is far from ideal. As an example of how a non-ideal omnidirectional antenna performs in comparison to an ideal one, we see in Fig. 4 that 1×1 $A1$ (at both Tx and Rx) system has much lower worst-case sum-SNR than 1×1 $A0$, despite that both antenna types have the same average power gain in the azimuth plane. The ABN/ASN can be used to improve the

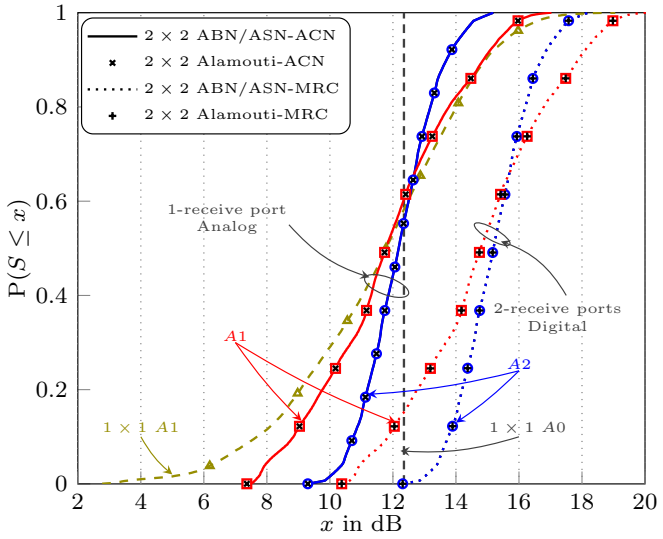

Fig. 4. CDF corresponding to the normalized sum-SNR of $K = 4$ packets, for different antennas and signal processing choices. The CDFs are computed for uniform AOA, AOD.

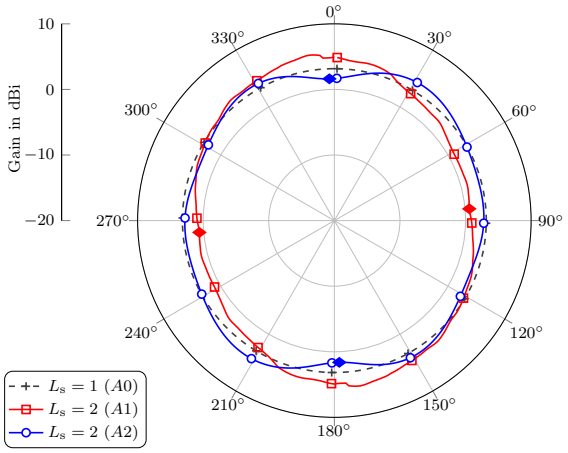

Fig. 5. Equivalent radiation pattern realized at the transmitter side using ABN/ASN for 2 elements of either $A1$ or $A2$ antennas. The elements are pointing 180 deg apart (i.e., $g_0^{\rm s}(\phi^{\rm s}) = g_1^{\rm s}(\phi^{\rm s} - 180)$). Worst-case AODs are marked with diamonds.

performance of a system based on such non-ideal antennas as well. In particular, an improvement of around 4.5 dB in worst-case sum-SNR is achieved using 2×2 $A1$ ABN/ASN system compared to 1×1 $A1$ system. This entails that ABN/ASN results in improved robustness of the system, which is also evident from the improved omnidirectional characteristics of the resultant equivalent radiation pattern at the Tx side, shown in Fig. 5.

Given access to more than one digital receive port and MRC processing, the ABN/ASN sum-SNR can be enhanced by 3 dB for all AOA, AOD. This can be seen from the 3 dB shifted CDF of ABN/ASN-MRC shown in Fig. 4 compared to ABN/ASN-ACN CDF. This 3 dB gain is in accordance with (65) when setting $L_{{\rm r},p} = 1$, $p = 0, 1$. From another aspect, we recall that an ABN/ASN has the same performance as an Alamouti scheme. Therefore, given access to two digital

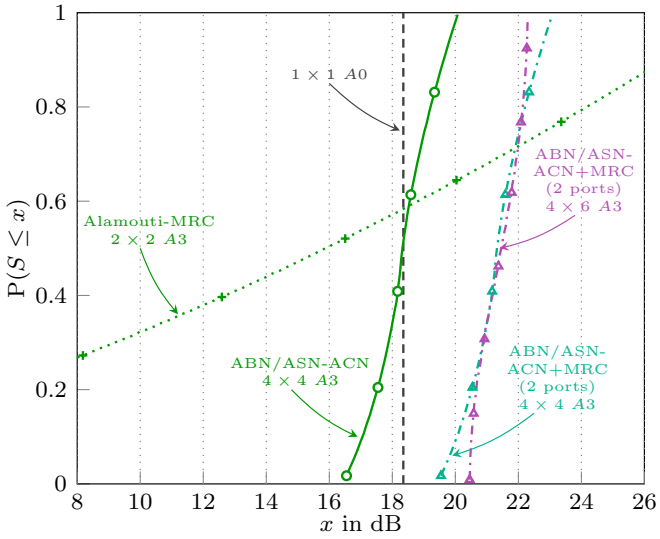

Fig. 6. CDF corresponding to the normalized sum-SNR of $K = 16$ packets, using $A3$ directional antennas. The CDFs are computed for uniform AOA, AOD. Antenna elements are pointing 180 deg and 90 deg apart, for the 2×2 and 4×4 systems, respectively. Antennas are divided equally among the two ports $L_{{\rm r},p} = 2$, $p = 0, 1$, for the hybrid receiver (ACN+MRC).

transmit ports, and as shown by the CDFs of Alamouti, no enhanced performance is achieved compared to ABN/ASN in this case.

To shed more light on the performance of ABN/ASN-ACN, we let $K = 16$ and we plot the CDF of the normalized sum-SNR for different $A3$ antenna systems in Fig. 6. We see that the performance of the 2×2 Alamouti-MRC system is poor, which is natural since two $A3$ antennas do not fully cover the azimuth plane. We cannot employ more than two antennas (without analog combining) in the Alamouti-MRC system, since we only have two digital ports. However, using ABN/ASN-ACN we can employ more antennas than available ports as long as $L_{\rm r} L_{\rm s} \leq K$. Following that, we see in Fig. 6 that the use of four $A3$ antennas at both ends yields a higher worst-case sum-SNR compared to Alamouti-MRC. Furthermore, combining ACN with a two-port MRC results in an additional 3 dB performance enhancement. Finally, using 6 receive antennas the worst-case sum-SNR is further improved by around 1 dB (the hybrid receiver allows the use of up to 8 receive antennas, $L_{{\rm r},p} = 8/2 = 4$, $p = 0, 1$). This latter gain is due to the improvement of the equivalent radiation pattern characteristics of the system.

B. On Optimality of Phase Slopes

In Theorem 1 we derived the optimality condition (30). To get insight into it, we plot in Fig. 7 the sum-SNR of a 2×2 ABN system based on $A2$ antennas as a function of the transmitter phase slopes for a fixed AOA, AOD (recall that Theorem 1 holds for any $(\phi^{\rm r}, \phi^{\rm s})$). An ACN with phase slopes vector that satisfies (30a) is used. In particular, the ACN vector is chosen according to (32), (46), so it is optimal for ASN as well. In the same figure, we also plot the sum-SNR for the ASN as a reference. Since ASN does not depend on the transmitter phase slopes, it maintains optimal performance. As

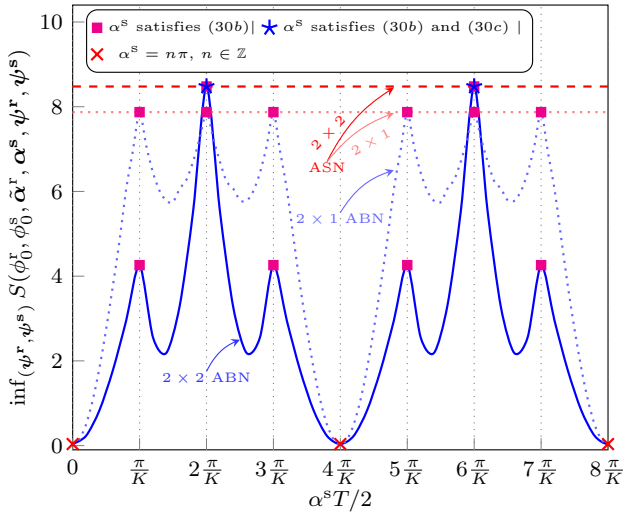

Fig. 7. Normalized sum-SNR of $K = 4$ packets of ABN and ASN as a function of $\boldsymbol{\alpha}^{\mathrm{s}} = [0, \alpha^{\mathrm{s}}]^{\mathsf{T}}$ when $L_{\mathrm{s}} = 2$ $(A2)$, and $L_{\mathrm{r}} = 2$ $(A2)$ with $\boldsymbol{\alpha}^{\mathrm{r}} = [0, 2\pi/KT]^{\mathsf{T}}$, or $L_{\mathrm{r}} = 1$ $(A2)$. The AOA, AOD are fixed to $(\phi_0^{\mathrm{r}}, \phi_0^{\mathrm{s}}) = (178, 178)$ deg.

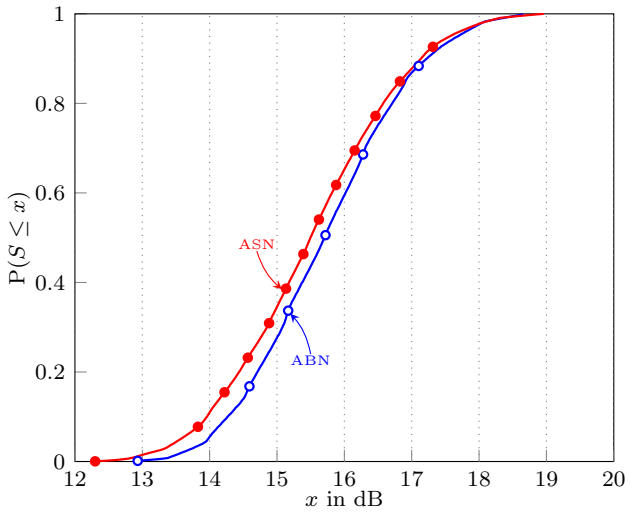

Fig. 8. CDF corresponding to the normalized sum-SNR of $K = 9$ packets of ABN and ASN (47), $L_{\mathrm{r}} = 2$, $L_{\mathrm{s}} = 2$. The CDFs are computed for uniform AOA, AOD.

for the 2×2 ABN, we can observe that when only (30b) is satisfied, a suboptimal performance is achieved. Optimality is ensured, however, when both (30b) and (30c) are met, which is in accordance with the results of Theorem 1. In comparison to 2×1 ABN, we see that at the points where (30b) is satisfied, optimal performance is achieved. Thus, employing multiple antennas at both Tx and Rx reduces the set of optimal phase slope points. Consequently, we see in the figure that for a large deviation from the optimal phase slopes, the relative sum-SNR loss is larger for the 2×2 than the 2×1 system. Yet, for a small phase slope mismatch, the relative loss is small for both systems. Curves showing the effect of ACN phase slopes mismatch on the sum-SNR of both ABN and ASN follow similar trends, and they are omitted for clarity. Since ASN-ACN depends only on phase slopes at the receiver, then it is less susceptible to the effects of mismatch in phase slopes compared to ABN-ACN.

C. ASN Performance when $K/L_{\mathrm{s}} \notin \mathbb{Z}$

As stated in Section III-B3, in the case $K/L_{\mathrm{s}} \notin \mathbb{Z}$, ASN is not known to achieve the optimal performance attained by ABN, when ACN phase slopes are set according to (46) (the phase slopes are optimal for ASN when $L_{\mathrm{s}}/K \in \mathbb{Z}$, and for ABN). In such a case, ASN performance is governed by (47), to which we do not have an available analytical solution. To quantify this numerically, we consider a burst of $K = 9$ packets, and a communication link between a transmitting VU with $L_{\mathrm{s}} = 2$ and a reference receiving VU with $L_{\mathrm{r}} = 2$. Both Tx and Rx use $A2$ antennas. In Fig. 8 we show the CDFs of the achieved sum-SNR when the transmitting VU is employing ASN or ABN, while the receiving VU is employing an ACN (following (46)). We observe that ASN achieves a suboptimal performance when $K/L_{\mathrm{s}} \notin \mathbb{Z}$. Yet, for this particular antenna system, the performance is negligibly lower (by around 0.5 dB) than the optimal ABN worst-case sum-SNR.

VI. Conclusions and Future Works

A fully analog, low-complexity, multiple antenna system for cooperative, periodic, broadcast V2V communication has been presented. Given that vehicular users (VUs) use an ACN [4] with L_{r} antennas at the receiver, we proposed the use of a network of phase shifters, ABN, or a network of switches, ASN, with L_{s} antennas at the transmitter. The overall system has been optimized, in absence of channel knowledge, to maximize the sum-SNR of K consecutive packets for the worst receiving VU (which minimizes the burst error probability when the packet error probability decreases exponentially with the per-packet SNR). The main findings of this work follow.

- Optimal sets of phase slopes for ABN (30), and for ASN (45) are derived when $L_{\mathrm{r}}L_{\mathrm{s}} \leq K$. The phase slopes are found to be independent of the far field functions of antennas. Moreover, the receiver phase slopes are consistent with what was found in [4].
- Both ABN and ASN yield the same optimal sum-SNR in the general case. For the special case of $L_{\mathrm{s}} = 2$ transmit antennas, the sum-SNR is equivalent to what can be achieved using an Alamouti diversity scheme.
- Given the maximum number of receive antennas a VU can have, $L_{\mathrm{r,max}}$, the ABN can be designed to achieve optimal performance for any user with $L_{\mathrm{r}} \leq L_{\mathrm{r,max}}$, including the worst receiving user. The ASN on the other hand does not require knowledge of $L_{\mathrm{r,max}}$, and it achieves optimal performance as long as L_{s} divides K.
- An ACN receiver can be designed to communicate optimally with both ABN and ASN transmitters.
- The derived phase slopes for ABN/ASN structures guarantee optimal sum-SNR also for a hybrid analog-digital ACN+MRC combiner.

In this work, to ensure a robust multiple-antenna system, ABN/ASN-ACN has been designed to achieve optimal sum-SNR under worst-case propagation scenario. This was

modeled by a sparse multipath propagation with a dominant path and a narrow angular spread, which tends to occur on roads that are not surrounded by buildings, e.g., highways. In future studies, it is important to also investigate the system performance under rich multipath propagation with wide angular spread, which is typical in urban scenarios. In addition, and since interference from other transmitting vehicles is prominent in such scenarios, its effect has to be taken into account in the investigation of ABN/ASN-ACN performance.

APPENDIX A
PROOF OF THEOREM 1

A. Notation

For convenience, we introduce the following notation. For an N-vector $\boldsymbol{v} = [v_0, v_1, \cdots, v_{N-1}]^{\mathsf{T}}$ we define the $(N-1)$-vector $\bar{\boldsymbol{v}}_n$ as

$$\bar{\boldsymbol{v}}_n \triangleq [v_0, v_1, \cdots, v_{n-1},\ v_{n+1}, \cdots, v_{N-1}]^{\mathsf{T}}. \tag{66}$$

We define the "averaging" operator $\mathcal{A}$ as an integral of a function with respect to variables $\boldsymbol{y} \in [0, 2\pi)^{L_\mathrm{r}}$ and $\boldsymbol{v} \in [0, 2\pi)^{L_\mathrm{s}}$, such that

$$\mathcal{A}[h(\boldsymbol{y}, \boldsymbol{v})] \triangleq \int_{[0,2\pi)^{L_\mathrm{s}}} \int_{[0,2\pi)^{L_\mathrm{r}}} h(\boldsymbol{y}, \boldsymbol{v})\, d\boldsymbol{y} d\boldsymbol{v}. \tag{67}$$

If we restrict the integration to be over just $\boldsymbol{y}$ or $\boldsymbol{v}$, we use the notation $\mathcal{A}_{\boldsymbol{y}}$ and $\mathcal{A}_{\boldsymbol{v}}$, respectively. We note that

$$\mathcal{A}[\cdot] = \mathcal{A}_{\boldsymbol{v}}\big[\mathcal{A}_{\boldsymbol{y}}[\cdot]\big] = \mathcal{A}_{\boldsymbol{y}}\big[\mathcal{A}_{\boldsymbol{v}}[\cdot]\big]. \tag{68}$$

Finally, we define

$$\mathcal{P}_\mathrm{r} \triangleq \{(l, i) : l, i \in \mathbb{Z}, 0 \le l < i \le L_\mathrm{r} - 1\}, \tag{69}$$

$$\mathcal{P}_\mathrm{s} \triangleq \{(m, j) : m, j \in \mathbb{Z}, 0 \le m < j \le L_\mathrm{s} - 1\}, \tag{70}$$

$$\Delta y_{l,i} \triangleq y_i - y_l. \tag{71}$$

Note that $\mathcal{P}_\mathrm{r} = \emptyset$ when $L_\mathrm{r} = 1$, and $\mathcal{P}_\mathrm{s} = \emptyset$ when $L_\mathrm{s} = 1$. In accordance with this, we use the convention

$$\sum_{e \in \mathcal{S}} c_e = 0, \quad \text{when } \ \mathcal{S} = \emptyset. \tag{72}$$

B. Preliminaries

For a fixed constant positive integer K we define the function $f : \mathbb{R}^2 \to \mathbb{R}$ as

$$f(x, y) \triangleq \sum_{k=0}^{K-1} \cos(y - 2kx). \tag{73}$$

Noting that $f(x, y) = \mathrm{Re}\{\mathrm{e}^{\jmath y} \sum_{k=0}^{K-1} \mathrm{e}^{-\jmath 2kx}\}$ and using the sum of geometric series, we get

$$f(x, y) = \begin{cases} K\cos(y), & x \in \mathcal{X} \\ \dfrac{\sin(Kx)}{\sin(x)} \cos\big(y - (K-1)x\big), & x \notin \mathcal{X} \end{cases} \tag{74}$$

where $\mathcal{X} \triangleq \{q\pi : q \in \mathbb{Z}\}$.

We state the following properties of $f(x, y)$:

(i) $f(x, y) = 0$ for all $y \in \mathbb{R}$, if and only if $x \in \mathcal{X}^*$, where

$$\mathcal{X}^* \triangleq \{q\pi/K : q \in \mathbb{Z}\} \setminus \mathcal{X}, \tag{75}$$

which follows from (74). Furthermore, we note that $x \in \mathcal{X}^* \Rightarrow x \notin \mathcal{X}$.

(ii) from the identity $2\cos(a)\cos(b) = \cos(a+b) + \cos(a-b)$ and (73), we deduce

$$2\sum_{k=0}^{K-1} \cos(y_1 - 2kx_1)\cos(y_2 - 2kx_2) = f(x_1 + x_2, y_1 + y_2) + f(x_1 - x_2, y_1 - y_2). \tag{76}$$

(iii) suppose a is a nonzero integer, then for all $x, B, C \in \mathbb{R}$,

$$\int_0^{2\pi} B f(x, ay + C)\, dy = 0, \tag{77}$$

which follows from (73).

Lemma 2. *Let $\boldsymbol{y} = [y_0, y_1, \cdots, y_{L_\mathrm{r}-1}]^{\mathsf{T}} \in [0, 2\pi)^{L_\mathrm{r}}$ and $\boldsymbol{v} = [v_0, v_1, \cdots, v_{L_\mathrm{s}-1}]^{\mathsf{T}} \in [0, 2\pi)^{L_\mathrm{s}}$. Then for $l, i \in \{0, 1, \cdots, L_\mathrm{r} - 1\}$ and $m, j \in \{0, 1, \cdots, L_\mathrm{s} - 1\}$*

$$\mathcal{A}_{\boldsymbol{y}}[f(x, \Delta y_{l,i} + C)] = 0, \quad l \ne i \tag{78}$$

$$\mathcal{A}_{\boldsymbol{v}}[f(x, \Delta v_{m,j} + C)] = 0, \quad m \ne j \tag{79}$$

$$\mathcal{A}[f(x, \Delta y_{l,i} + \Delta v_{m,j} + C)] = 0, \ \begin{cases} l \ne i, \text{ or} \\ m \ne j \end{cases} \tag{80}$$

where $x, C \in \mathbb{R}$.

Proof. Suppose $l \ne i$ we can write $f(x, \Delta y_{l,i} + \Delta v_{m,j} + C) = f(x, y_i + C')$, where $C' = -y_l + (v_j - v_m) + C$ is a constant with respect to y_i. Then, $\mathcal{A}_{\boldsymbol{y}}[f(x, \Delta y_{l,i} + \Delta v_{m,j} + C)]$ can be expressed as

$$\int_{[0,2\pi)^{L_\mathrm{r}-1}} \underbrace{\left[\int_{y_i \in [0,2\pi)} f(x, y_i + C')\, dy_i\right]}_{=\,0 \text{ according to (77)}} d\bar{\boldsymbol{y}}_i = 0,$$

which, together with (68), implies that (80) holds when $l \ne i$. It is straightforward to develop a similar argument based on $\mathcal{A}_{\boldsymbol{v}}[\cdot]$ to prove (80) when $m \ne j$. Moreover, (78) and (79) follow from (80) by considering $m = j$ and $l = i$, respectively, which completes the proof. □

Lemma 3. *Let $\boldsymbol{y} = [y_0, y_1, \cdots, y_{L_\mathrm{r}-1}]^{\mathsf{T}} \in [0, 2\pi)^{L_\mathrm{r}}$ and $\boldsymbol{v} = [v_0, v_1, \cdots, v_{L_\mathrm{s}-1}]^{\mathsf{T}} \in [0, 2\pi)^{L_\mathrm{s}}$. For $w, w' \in \mathcal{P}_r$ and $u, u' \in \mathcal{P}_s$, we have*

$$\mathcal{A}_{\boldsymbol{y}}[f(x_1, C_1 \pm \Delta y_w) f(x_2, C_2 \pm \Delta y_{w'})] = 0, \ w \ne w' \tag{81}$$

$$\mathcal{A}_{\boldsymbol{v}}[f(x_1, C_1 \pm \Delta v_u) f(x_2, C_2 \pm \Delta v_{u'})] = 0, \ u \ne u' \tag{82}$$

$$\mathcal{A}[f(x_1, \Delta y_w + a\Delta v_u) f(x_2, \Delta y_{w'} + a\Delta v_{u'})] = 0, \quad a = \pm 1, \ w \ne w' \text{ or } u \ne u' \tag{83}$$

$$\mathcal{A}[f(x_1, \Delta y_w + \Delta v_u) f(x_2, \Delta y_{w'} - \Delta v_{u'})] = 0, \tag{84}$$

$$\mathcal{A}_{\boldsymbol{y}}[f(x_1, \Delta y_w \pm \Delta v_u) f(x_2, \Delta v_{u'})] = 0, \tag{85}$$

$$\mathcal{A}_{\boldsymbol{v}}[f(x_1, \Delta y_w \pm \Delta v_u) f(x_2, \Delta y_{w'})] = 0, \tag{86}$$

$$\mathcal{A}[f(x_1, \Delta y_w) f(x_2, \Delta v_u)] = 0, \tag{87}$$

where $x_1, x_2, C_1, C_2 \in \mathbb{R}$.

Proof. Let $w = (l, i)$, $w' = (r, q)$, $u = (m, j)$ and $u' = (t, s)$ throughout this proof. Given that $w, w' \in \mathcal{P}_\mathrm{r}$, and $u, u' \in \mathcal{P}_\mathrm{s}$, it follows that $l < i$, $r < q$, $m < j$, and $t < s$.

Let us start by proving (81). Suppose $w \neq w'$, i.e., $(l,i) \neq (r,q)$, which implies that $l \neq r$ or $i \neq q$. Let us consider these two cases separately.

(i) Suppose that $l \neq r$. Then either $l < r$ or $r < l$, which (since $l < i$ and $r < q$) implies that $n = \min\{l,r\}$ is the unique minimum element in the multiset $[l,i,r,q]$. Hence, the integration variable y_n appears in the argument of either $f(x_1, C_1 \pm \Delta y_w) = f(x_1, C_1 \pm \Delta y_{l,i}) = f(x_1, C_1 \pm (y_i - y_l))$ or $f(x_2, C_2 \pm \Delta y_{w'}) = f(x_2, C_2 \pm \Delta y_{r,q}) = f(x_2, C_2 \pm (y_q - y_r))$, but not in both. Then, the integrand in (81) can be expressed as

$$Bf(x', C' - ay_n),\ a = \pm 1$$

where $B = f(x_2, C_2 \pm \Delta y_{r,q})$, $C' = C_1 + ay_i$ and $x' = x_1$ if $n = l$, while $B = f(x_1, C_1 \pm \Delta y_{l,i})$, $C' = C_2 + ay_q$ and $x' = x_2$ if $n = r$. Note that in both cases B and C' are constants with respect to y_n. Hence, the left-hand side of (81) satisfies

$$\int_{[0,2\pi)^{L_\mathrm{r}-1}} \underbrace{\left[\int_{y_n \in [0,2\pi)} Bf(x', C' - ay_n) dy_n\right]}_{=0 \text{ according to (77)}} d\bar{\boldsymbol{y}}_n = 0,$$

and thus, (81) holds when $l \neq r$.

(ii) Suppose that $i \neq q$. Then either $i > q$ or $q > i$, which implies that $n = \max\{i,q\}$ is the unique maximum element in the multiset $[l,i,r,q]$. Hence, just as in case (i), the integration variable y_n appears in the argument of either $f(x_1, C_1 \pm (y_i - y_l))$ or $f(x_2, C_2 \pm (y_q - y_r))$, but not in both. Hence, (81) holds also when $i \neq q$.

Combining the results of (i) and (ii) proves that (81) holds. Moreover, the same basic arguments, (i) and (ii), can be repeated to prove (82).

Now, consider the integrand in (83). When integrating over $\boldsymbol{y}$ ($\mathcal{A}_{\boldsymbol{y}}[\cdot]$), it can be expressed as

$$f(x_1, \Delta y_w + C_1) f(x_2, \Delta y_{w'} + C_2),$$

where $C_1 = a\Delta v_u = a\Delta v_{m,j} = a(v_j - v_m)$ and $C_2 = a\Delta v_{u'} = a\Delta v_{t,s} = a(v_s - v_t)$ are constants and $a = \pm 1$. Hence, it follows from (81) and the decomposition $\mathcal{A}[\cdot] = \mathcal{A}_{\boldsymbol{v}}\big[\mathcal{A}_{\boldsymbol{y}}[\cdot]\big]$ that (83) holds when $w \neq w'$. On the other hand, by starting the integration over $\boldsymbol{v}$, then employing (82) and $\mathcal{A}[\cdot] = \mathcal{A}_{\boldsymbol{y}}\big[\mathcal{A}_{\boldsymbol{v}}[\cdot]\big]$, we deduce that (83) holds also when $u \neq u'$, which completes the proof of (83).

By similar argument to what was presented to demonstrate (83), we can show that (84) holds when $w \neq w'$ or $u \neq u'$. For the case $w = w'$ and $u = u'$, i.e., $(l,i) = (r,q)$ and $(m,j) = (t,s)$, the integrand of (84) can be expressed based on (73) and the identity $2cos(a)cos(b) = cos(a+b) + cos(a-b)$ as

$$\frac{1}{2}\sum_{k=0}^{K-1}\sum_{k'=0}^{K-1} \cos(2\Delta y_{l,i} - 2(kx_1 + k'x_2)) + \cos\big(2\Delta v_{m,j} - 2(kx_1 - k'x_2)\big). \tag{88}$$

Integrating (88) with respect to $\boldsymbol{y}$ and $\boldsymbol{v}$ yields zero, and this completes the proof of (84).

Since Δv_u and $f(x_2, \Delta v_{u'})$ are constants with respect to $\boldsymbol{y}$, the left-hand side of (85) can be written as

$$f(x_2, \Delta v_{u'}) \mathcal{A}_{\boldsymbol{y}}[f(x_1, \Delta y_w + C)],$$

where $C = \pm \Delta v_u$, and it follows directly from Lemma 2, (78) ($w = (l,i)$, $l < i$) that (85) holds. By similar argument (86) follows from Lemma 2, (79). Finally, employing the decomposition (68), (87) follows from Lemma 2, (78) or (79) and this completes the lemma proof. □

C. Proof of Theorem 1 and Corollary 1

Given the objective function $S_\mathrm{a}(\phi^\mathrm{r}, \phi^\mathrm{s}, \boldsymbol{\alpha}^\mathrm{r}, \boldsymbol{\alpha}^\mathrm{s}, \boldsymbol{\psi}^\mathrm{r}, \boldsymbol{\psi}^\mathrm{s})$, defined in (22), where $L_\mathrm{r} \geq 1$, $L_\mathrm{s} \geq 1$, and $L_\mathrm{r} + L_\mathrm{s} > 2$ (the trivial case $L_\mathrm{r} = L_\mathrm{s} = 1$ is omitted). We define L_r-vectors $\boldsymbol{x} \in \mathbb{R}^{L_\mathrm{r}}$ and $\boldsymbol{y} \in [0,2\pi)^{L_\mathrm{r}}$ with elements $x_l \triangleq \alpha_l^\mathrm{r} T/2$ and $y_l \triangleq \psi_l^\mathrm{r}$, $0 \leq l \leq L_\mathrm{r} - 1$. Analogously, we define L_s-vectors $\boldsymbol{z} \in \mathbb{R}^{L_\mathrm{s}}$ and $\boldsymbol{v} \in [0,2\pi)^{L_\mathrm{s}}$ with elements $z_m \triangleq \alpha_m^\mathrm{s} T/2$ and $v_m \triangleq \psi_m^\mathrm{s}$, $0 \leq m \leq L_\mathrm{s} - 1$. Last, we let $\boldsymbol{\phi} \triangleq (\phi^\mathrm{r}, \phi^\mathrm{s})$. The objective function can be expressed using this notation as

$$S_\mathrm{a}(\boldsymbol{\phi}, \boldsymbol{x}, \boldsymbol{z}, \boldsymbol{y}, \boldsymbol{v}) = K\overline{G}(\boldsymbol{\phi}) + J_\mathrm{a}(\boldsymbol{\phi}, \boldsymbol{x}, \boldsymbol{z}, \boldsymbol{y}, \boldsymbol{v}), \tag{89}$$

where J_a is given by (25). Using the definitions of f, $\mathcal{P}_\mathrm{r}$, and $\mathcal{P}_\mathrm{s}$, we can express J_a as

$$\begin{aligned} &J_\mathrm{a}(\boldsymbol{\phi}, \boldsymbol{x}, \boldsymbol{z}, \boldsymbol{y}, \boldsymbol{v}) = \\ &\overbrace{\sum_{w \in \mathcal{P}_\mathrm{r}} c_w f(\Delta x_w, \Delta y_w)}^{J_\mathrm{a}^\mathrm{r}} + \overbrace{\sum_{u \in \mathcal{P}_\mathrm{s}} d_u f(\Delta z_u, \Delta v_u)}^{J_\mathrm{a}^\mathrm{s}} \\ &+ \sum_{w \in \mathcal{P}_\mathrm{r}} \sum_{u \in \mathcal{P}_\mathrm{s}} 0.5 c'_w d'_u f(\Delta x_w + \Delta z_u, \Delta y_w + \Delta v_u) \\ &+ \sum_{w \in \mathcal{P}_\mathrm{r}} \sum_{u \in \mathcal{P}_\mathrm{s}} 0.5 c'_w d'_u f(\Delta x_w - \Delta z_u, \Delta y_w - \Delta v_u), \end{aligned} \tag{90}$$

where the last two terms follow from (76). The dependency of the nonnegative coefficients c_w, c'_w, d_u, d'_u—defined in (26)—on $\boldsymbol{\phi}$ is dropped for convenience. Note that, in the special case of $L_\mathrm{r} = 1$, $\mathcal{P}_\mathrm{r} = \emptyset$ and with reference to the convention (72), we get $J_\mathrm{a} = J_\mathrm{a}^\mathrm{s}$, while when $L_\mathrm{s} = 1$, $\mathcal{P}_\mathrm{s} = \emptyset$, we get $J_\mathrm{a} = J_\mathrm{a}^\mathrm{r}$.

We observe that $J_\mathrm{a}(\boldsymbol{\phi}, \boldsymbol{x}, \boldsymbol{z}, \boldsymbol{y}, \boldsymbol{v})$ is a linear combination of f-functions with nonnegative coefficients—a crucial property for the proof to follow. The proof is divided into three lemmas which are presented first, then follows the demonstration of the theorem claims at last.

Lemma 4. *Let J_a be defined as in* (90) *where $\boldsymbol{x} \in \mathbb{R}^{L_\mathrm{r}}$, $\boldsymbol{y} \in [0,2\pi)^{L_\mathrm{r}}$, $\boldsymbol{z} \in \mathbb{R}^{L_\mathrm{s}}$, and $\boldsymbol{v} \in [0,2\pi)^{L_\mathrm{s}}$. Then,*

$$\mathcal{A}[J_\mathrm{a}(\boldsymbol{\phi}, \boldsymbol{x}, \boldsymbol{z}, \boldsymbol{y}, \boldsymbol{v})] = 0, \tag{91}$$

$$\inf_{\boldsymbol{y} \in [0,2\pi)^{L_\mathrm{r}}, \boldsymbol{v} \in [0,2\pi)^{L_\mathrm{s}}} J_\mathrm{a}(\boldsymbol{\phi}, \boldsymbol{x}, \boldsymbol{z}, \boldsymbol{y}, \boldsymbol{v}) \leq 0. \tag{92}$$

Proof. From (90) we see that $J_\mathrm{a}(\boldsymbol{\phi}, \boldsymbol{x}, \boldsymbol{z}, \boldsymbol{y}, \boldsymbol{v})$ is a linear combination of f-functions with nonnegative coefficients. The f-functions are of the general form $f(x, a\Delta y_w + b\Delta v_u) = f(x, a\Delta y_{l,i} + b\Delta v_{m,j})$, where $a, b \in \{0, \pm 1\}$ and they are not both zero at the same time. This is valid in the general case of $L_\mathrm{r} > 1, L_\mathrm{s} > 1$, as well as in the special cases of $L_\mathrm{r} = 1$ ($a = 0$, $b = 1$), or $L_\mathrm{s} = 1$ ($a = 1$, $b = 0$). Since $w = (l,i) \in \mathcal{P}_\mathrm{r}$ and $u = (m,j) \in \mathcal{P}_\mathrm{s}$, we have

that $i \neq l$ and $j \neq m$, and $\mathcal{A}[f(x, a\Delta y_{l,i} + b\Delta v_{m,j})] = 0$ according to Lemma 2 and (68). We recall that $\mathcal{A}[\cdot]$ is an integral over the same domain as over which the infimum is taken in (92), namely $\boldsymbol{y} \in [0, 2\pi)^{L_\mathrm{r}}, \boldsymbol{v} \in [0, 2\pi)^{L_\mathrm{s}}$. Hence, $\mathcal{A}[f(x, a\Delta y_{l,i} + b\Delta v_{m,j})] = 0$ implies that

$$0 = \mathcal{A}[J_\mathrm{a}(\boldsymbol{\phi}, \boldsymbol{x}, \boldsymbol{z}, \boldsymbol{y}, \boldsymbol{v})] \tag{93}$$

$$\geq \mathcal{A}\left[\inf_{\boldsymbol{y}\in[0,2\pi)^{L_\mathrm{r}}, \boldsymbol{v}\in[0,2\pi)^{L_\mathrm{s}}} J_\mathrm{a}(\boldsymbol{\phi}, \boldsymbol{x}, \boldsymbol{z}, \boldsymbol{y}, \boldsymbol{v})\right] \tag{94}$$

$$= (2\pi)^{L_\mathrm{r}+L_\mathrm{s}} \inf_{\boldsymbol{y}\in[0,2\pi)^{L_\mathrm{r}}, \boldsymbol{v}\in[0,2\pi)^{L_\mathrm{s}}} J_\mathrm{a}(\boldsymbol{\phi}, \boldsymbol{x}, \boldsymbol{z}, \boldsymbol{y}, \boldsymbol{v}), \tag{95}$$

where the last equality holds since $\mathcal{A}[C] = C(2\pi)^{L_\mathrm{r}+L_\mathrm{s}}$ for a constant C, and the lemma therefore follows. □

Lemma 5. *Let J_a be as defined in* (90)*, where $\boldsymbol{x} \in \mathbb{R}^{L_\mathrm{r}}$, $\boldsymbol{y} \in [0, 2\pi)^{L_\mathrm{r}}$, $\boldsymbol{z} \in \mathbb{R}^{L_\mathrm{s}}$, and $\boldsymbol{v} \in [0, 2\pi)^{L_\mathrm{s}}$. Let $\mathcal{X}^*$ be as defined in* (75)*, and*

$$\begin{aligned}\mathcal{D}_X &\triangleq \{\Delta x_w, \Delta z_u, \Delta x_w \pm \Delta z_u : w \in \mathcal{P}_r, u \in \mathcal{P}_s\} \\ &= \{\Delta z_u : u \in \mathcal{P}_s, \mathcal{P}_r = \emptyset\} \\ &= \{\Delta x_w : w \in \mathcal{P}_r, \mathcal{P}_s = \emptyset\}.\end{aligned} \tag{96}$$

(i) If $\mathcal{D}_X \subset \mathcal{X}^*$ then

$$J_\mathrm{a}(\boldsymbol{\phi}, \boldsymbol{x}, \boldsymbol{z}, \boldsymbol{y}, \boldsymbol{v}) = 0, \quad \boldsymbol{y} \in [0, 2\pi)^{L_\mathrm{r}}, \boldsymbol{v} \in [0, 2\pi)^{L_\mathrm{s}}. \tag{97}$$

(ii) Assuming that $c_w, c'_w, d_u, d'_u > 0$, $w \in \mathcal{P}_r$, $u \in \mathcal{P}_s$, then (97) $\implies \mathcal{D}_X \subset \mathcal{X}^*$.

Proof. (i) We see from (90) that J_a is a linear combination of terms of the form $f(\Delta_X, \Delta_Y)$, where $\Delta_X \in \mathcal{D}_X$ defined in (96), and $\Delta_Y \in \mathcal{D}_Y$,

$$\begin{aligned}\mathcal{D}_Y &\triangleq \{\Delta y_w, \Delta v_u, \Delta y_w \pm \Delta v_u : w \in \mathcal{P}_\mathrm{r}, u \in \mathcal{P}_\mathrm{s}\} \\ &= \{\Delta v_u : u \in \mathcal{P}_\mathrm{s}, \mathcal{P}_\mathrm{r} = \emptyset\} \\ &= \{\Delta y_w : w \in \mathcal{P}_\mathrm{r}, \mathcal{P}_\mathrm{s} = \emptyset\}.\end{aligned} \tag{98}$$

Suppose $\mathcal{D}_X \subset \mathcal{X}^*$, then $\Delta_X \in \mathcal{D}_X \subset \mathcal{X}^*$, which together with (75) implies that $f(\Delta_X, \Delta_Y) = 0$ for all $\Delta_Y \in \mathbb{R}$, which in turn implies that (97) hold. In other words, $\mathcal{D}_X \subset \mathcal{X}^* \Rightarrow$ (97).

(ii) Suppose (97) holds, then $J_\mathrm{a}^2 = 0$, which implies that $\mathcal{A}[J_\mathrm{a}^2] = 0$. From (90), we see that J_a^2 can be written as a linear combinations of terms of the form $f(\Delta_X, \Delta_Y)f(\Delta'_X, \Delta'_Y)$, where $\Delta_X, \Delta'_X \in \mathcal{D}_X$ and $\Delta_Y, \Delta'_Y \in \mathcal{D}_Y$. From Lemma 3, we can see that $\mathcal{A}[f(\Delta_X, \Delta_Y)f(\Delta'_X, \Delta'_Y)] = 0$ when $\Delta_Y \neq \Delta'_Y$. Hence, it follows from (90) that

$$\begin{aligned}&\mathcal{A}[J_\mathrm{a}^2] = \mathcal{A}[\xi] + \\ &\mathcal{A}\left[\sum_{w\in\mathcal{P}_\mathrm{r}} c_w^2 f^2(\Delta x_w, \Delta y_w) + \sum_{u\in\mathcal{P}_\mathrm{s}} d_u^2 f^2(\Delta z_u, \Delta v_u)\right. \\ &\quad + \sum_{w\in\mathcal{P}_\mathrm{r}}\sum_{u\in\mathcal{P}_\mathrm{s}} \frac{(c'_w d'_u)^2}{4} f^2(\Delta x_w + \Delta z_u, \Delta y_w + \Delta v_u) \\ &\quad \left. + \sum_{w\in\mathcal{P}_\mathrm{r}}\sum_{u\in\mathcal{P}_\mathrm{s}} \frac{(c'_w d'_u)^2}{4} f^2(\Delta x_w - \Delta z_u, \Delta y_w - \Delta v_u)\right],\end{aligned} \tag{99}$$

where $\mathcal{A}[\xi] = 0$ accounts for all cross-terms, i.e., the terms when $\Delta_Y \neq \Delta'_Y$. Note that in the special case of $L_\mathrm{r} = 1$, $\mathcal{P}_\mathrm{r} = \emptyset$ and following the convention (72), $A[J_\mathrm{a}^2] = \sum_{u\in\mathcal{P}_\mathrm{s}} d_u^2\ \mathcal{A}[f^2(\Delta z_u, \Delta v_u)]$, while for the special case $L_\mathrm{s} = 1$, $A[J_\mathrm{a}^2] = \sum_{w\in\mathcal{P}_\mathrm{r}} c_w^2\ \mathcal{A}[f^2(\Delta x_w, \Delta y_w)]$.

The squared f-functions in (99) are of the form $f^2(\Delta_X, \Delta_Y)$, where $\Delta_X \in \mathcal{D}_X$ and $\Delta_Y \in \mathcal{D}_Y$. We note that not all combinations of $\Delta_X \in \mathcal{D}_X$ and $\Delta_Y \in \mathcal{D}_Y$ are present in (99), but will not make this dependency notationally explicit. Now, with this abuse of notation, given (99) and the assumption that c_w, c'_w, d_u, $d'_u > 0$, are positive reals, $\mathcal{A}[J_\mathrm{a}^2] = 0$ holds, if and only if

$$\mathcal{A}[f^2(\Delta_X, \Delta_Y)] = 0, \qquad \Delta_X \in \mathcal{D}_X, \Delta_Y \in \mathcal{D}_Y. \tag{100}$$

Recalling (74), $f^2(\Delta_X, \Delta_Y)$ is equal to

$$\begin{cases} K^2\cos^2(\Delta_Y), & \Delta_X \in \mathcal{X} \\ \dfrac{\sin^2(K\Delta_X)}{\sin^2(\Delta_X)}\cos^2\big(\Delta_Y - (K-1)\Delta_X\big), & \Delta_X \notin \mathcal{X}. \end{cases}$$

We also recall that $\mathcal{A}[f^2(\Delta_X, \Delta_Y)]$ is an integral over the domain $\boldsymbol{y} \in [0, 2\pi)^{L_\mathrm{r}}, \boldsymbol{v} \in [0, 2\pi)^{L_\mathrm{s}}$, i.e., with respect to variables in Δ_Y. Hence, $\mathcal{A}[f^2(\Delta_X, \Delta_Y)]$ is proportional to the integral $\mathcal{A}[\cos^2(\Delta_Y + C)]$ for a constant C. Now, since $2\cos^2(a) = 1 + \cos(2a)$ and $\mathcal{A}[1] = (2\pi)^{L_\mathrm{s}+L_\mathrm{r}}$,

$$\mathcal{A}[\cos^2(\Delta_Y + C)] = \frac{1}{2}(2\pi)^{L_\mathrm{s}+L_\mathrm{r}} + \frac{1}{2}\mathcal{A}[\cos(2\Delta_Y + 2C)].$$

The latter integral is zero, since $\Delta_Y \in \mathcal{D}_Y$ contains at least two independent integration variables (e.g., $\Delta_Y = \Delta v_u = \Delta v_{m,j} = v_m - v_j$), and therefore $\mathcal{A}[\cos(2\Delta_Y + 2C)] = 0$. We have now shown that

$$\mathcal{A}[f^2(\Delta_X, \Delta_Y)] = \begin{cases} \dfrac{1}{2}(2\pi)^{L_\mathrm{s}+L_\mathrm{r}}K^2, & \Delta_X \in \mathcal{X} \\ \dfrac{1}{2}(2\pi)^{L_\mathrm{s}+L_\mathrm{r}}\dfrac{\sin^2(K\Delta_X)}{\sin^2(\Delta_X)}, & \Delta_X \notin \mathcal{X} \end{cases}$$

which is zero, if and only if $\Delta_X \in \mathcal{X}^*$, and thus (100) $\iff$ $\mathcal{D}_X \subset \mathcal{X}^*$.

Putting our argument in order, (97) $\Rightarrow \mathcal{A}[J_\mathrm{a}^2] = 0$, and under the assumption that c_w, c'_w, d_u, $d'_u > 0$, $\mathcal{A}[J_\mathrm{a}^2] = 0$ $\iff$ (100) $\iff$ $\mathcal{D}_X \subset \mathcal{X}^*$. Therefore, we conclude that (97) $\Rightarrow \mathcal{D}_X \subset \mathcal{X}^*$, and the lemma follows. □

Lemma 6. *Let $\boldsymbol{x} \in \mathbb{R}^{L_\mathrm{r}}$, $\boldsymbol{z} \in \mathbb{R}^{L_\mathrm{s}}$, $\mathcal{D}_X$ be as defined in* (96) *and $\mathcal{X}^*$ as defined in* (75)*. Then,*

$$\exists(\boldsymbol{x}, \boldsymbol{z}) : \mathcal{D}_X \subset \mathcal{X}^* \iff L_\mathrm{r}L_\mathrm{s} \leq K. \tag{101}$$

One selection of elements that satisfies $\mathcal{D}_X \subset \mathcal{X}^*$ is

$$x_l = l\frac{\pi}{K}, \quad l = 0, 1, \cdots L_\mathrm{r} - 1, \tag{102a}$$

$$z_m = mL_\mathrm{r}\frac{\pi}{K}, \quad m = 0, 1, \cdots L_\mathrm{s} - 1. \tag{102b}$$

Proof. Before tackling the proof, we start by presenting some definitions and notation. We recall that $\mathcal{X}^* = \{q\pi/K : q \in \mathbb{Z}\} \setminus \{n\pi,\ n \in \mathbb{Z}\}$. Then, let us define the set

$$\mathcal{X}^{**} \triangleq \{a\pi/K : a \in \mathbb{Z}, 1 \leq a \leq K - 1\}, \tag{103}$$

which satisfies $\mathcal{X}^{**} \subset \mathcal{X}^*$ and

$$a \in \mathcal{X}^* \iff \mathrm{mod}(a, \pi) \in \mathcal{X}^{**}, \tag{104}$$

$$(a - b) \in \mathcal{X}^* \implies \mathrm{mod}(a, \pi) \neq \mathrm{mod}(b, \pi). \tag{105}$$

where $\mathrm{mod}(a,b)$ is the remainder of dividing a by b. The sum or subtraction of two sets is defined as

$$\mathcal{B} \pm \mathcal{C} = \{b \pm c : b \in \mathcal{B}, c \in \mathcal{C}\}. \tag{106}$$

Then, we define for $\boldsymbol{x}$ and $\boldsymbol{z}$ the sets

$$\mathcal{E}_{\Delta x} \triangleq \{\Delta x_{l,i} : (l,i) \in \mathcal{P}_{\mathrm{r}}\}, \qquad \text{If } \mathcal{P}_{\mathrm{r}} = \emptyset,\ \mathcal{E}_{\Delta x} = \emptyset. \tag{107}$$

$$\mathcal{E}_{\Delta z} \triangleq \{\Delta z_{m,j} : (m,j) \in \mathcal{P}_{\mathrm{s}}\}, \quad \text{If } \mathcal{P}_{\mathrm{s}} = \emptyset,\ \mathcal{E}_{\Delta z} = \emptyset. \tag{108}$$

From (96) we see that, when $L_{\mathrm{r}} > 1$, $L_{\mathrm{s}} > 1$ ($\mathcal{P}_{\mathrm{r}} \neq \emptyset$, $\mathcal{P}_{\mathrm{s}} \neq \emptyset$)

$$\mathcal{D}_X = \mathcal{E}_{\Delta x} \cup \mathcal{E}_{\Delta z} \cup (\mathcal{E}_{\Delta x} + \mathcal{E}_{\Delta z}) \cup (\mathcal{E}_{\Delta x} - \mathcal{E}_{\Delta z}), \tag{109}$$

while $\mathcal{D}_X = \mathcal{E}_{\Delta z}$, when $L_{\mathrm{r}} = 1$, and $\mathcal{D}_X = \mathcal{E}_{\Delta x}$ when $L_{\mathrm{s}} = 1$. Last, we introduce the set notation

$$\{N\}_{n_0}^{n_1} \triangleq \{N \in \mathbb{Z} : n_0 \leq N \leq n_1\}. \tag{110}$$

Now, we are set to tackle the proof. We start by showing that $L_{\mathrm{r}}L_{\mathrm{s}} \leq K \implies \exists(\boldsymbol{x},\boldsymbol{z}) : \mathcal{D}_X \subset \mathcal{X}^*$. Let $L_{\mathrm{r}}L_{\mathrm{s}} \leq K$, and let $\boldsymbol{x}$ and $\boldsymbol{z}$ be selected following (102). Then, for $(l,i) \in \mathcal{P}_{\mathrm{r}}$ and $(m,j) \in \mathcal{P}_{\mathrm{s}}$, we have $\Delta x_{l,i} = x_i - x_l = (i-l)\pi/K$, $0 \leq l < i \leq L_{\mathrm{r}} - 1$, and $\Delta z_{m,j} = z_j - z_m = (j-m)L_{\mathrm{r}}\pi/K$, $0 \leq m < j \leq L_{\mathrm{s}} - 1$. This implies

$$\mathcal{E}_{\Delta x} = \{a\pi/K : 1 \leq a \leq L_{\mathrm{r}} - 1\}, \tag{111}$$

$$\mathcal{E}_{\Delta z} = \{bL_{\mathrm{r}}\pi/K : 1 \leq b \leq L_{\mathrm{s}} - 1\}, \tag{112}$$

$$\mathcal{E}_{\Delta z} + \mathcal{E}_{\Delta x} = \Big\{(bL_{\mathrm{r}} + a)\frac{\pi}{K} : \{a\}_1^{L_{\mathrm{r}}-1}, \{b\}_1^{L_{\mathrm{s}}-1}\Big\}, \tag{113}$$

$$\mathcal{E}_{\Delta z} - \mathcal{E}_{\Delta x} = \Big\{(bL_{\mathrm{r}} - a)\frac{\pi}{K} : \{a\}_1^{L_{\mathrm{r}}-1}, \{b\}_1^{L_{\mathrm{s}}-1}\Big\}. \tag{114}$$

Since, $(L_{\mathrm{r}} - 1) \leq K - 1$, from (111) and (103) we deduce that $\mathcal{E}_{\Delta x} \subset \mathcal{X}^{**}$. Similarly, we have that in (112)–(114)

$$L_{\mathrm{r}} \leq bL_{\mathrm{r}} \quad \leq (L_{\mathrm{s}} - 1)L_{\mathrm{r}} \quad \leq K - 1, \tag{115}$$

$$L_{\mathrm{r}} + 1 \leq bL_{\mathrm{r}} + a \leq L_{\mathrm{r}}L_{\mathrm{s}} - 1 \quad \leq K - 1, \tag{116}$$

$$1 \leq bL_{\mathrm{r}} - a \leq (L_{\mathrm{s}} - 1)L_{\mathrm{r}} - 1 \leq K - 1. \tag{117}$$

It consequently follows by (103) that, also, $\mathcal{E}_{\Delta z}$, $\mathcal{E}_{\Delta z} + \mathcal{E}_{\Delta x}$, and $\mathcal{E}_{\Delta z} - \mathcal{E}_{\Delta x}$ are subsets of $\mathcal{X}^{**} \subset \mathcal{X}^*$. Note that $\mathcal{E}_{\Delta z} - \mathcal{E}_{\Delta x} \subset \mathcal{X}^*$ implies that $-(\mathcal{E}_{\Delta z} - \mathcal{E}_{\Delta x}) \subset \mathcal{X}^*$ (if $x \in \mathcal{X}^*$, $-x \in \mathcal{X}^*$). Recalling (109) we can conclude that $\mathcal{D}_X \subset \mathcal{X}^*$. Note that this holds in the special case of $L_{\mathrm{r}} = 1$ ($\mathcal{E}_{\Delta x} = \emptyset$), because $\mathcal{D}_X = \mathcal{E}_{\Delta z} \subset \mathcal{X}^*$, it also holds when $L_{\mathrm{s}} = 1$ ($\mathcal{E}_{\Delta z} = \emptyset$), for $\mathcal{D}_X = \mathcal{E}_{\Delta x} \subset \mathcal{X}^*$.

We have shown that when $L_{\mathrm{r}}L_{\mathrm{s}} \leq K$, (102) is a solution satisfying $\mathcal{D}_X \subset \mathcal{X}^*$, when $L_{\mathrm{r}} + L_{\mathrm{s}} > 2$, and thus the statement "$L_{\mathrm{r}}L_{\mathrm{s}} \leq K \implies \exists(\boldsymbol{x},\boldsymbol{z}) : \mathcal{D}_X \in \mathcal{X}^{**}$" holds.

Now we move to the second part of the claim of the lemma, $\exists(\boldsymbol{x},\boldsymbol{z}) : \mathcal{D}_X \in \mathcal{X}^* \implies L_{\mathrm{r}}L_{\mathrm{s}} \leq K$. We shall show that through a proof of contradiction. Assume that $L_{\mathrm{r}}L_{\mathrm{s}} > K$. By construction of the set $\mathcal{X}^{**}$ (103) we have that

$$|\mathcal{X}^{**}| = K - 1 < L_{\mathrm{r}}L_{\mathrm{s}} - 1, \qquad K < L_{\mathrm{r}}L_{\mathrm{s}}. \tag{118}$$

To form a contradiction, we proceed to find a lower bound on the cardinality of the set $\mathcal{X}^{**}$ assuming that there exists a solution $(\boldsymbol{x},\boldsymbol{z})$ that satisfies $\mathcal{D}_X \subset \mathcal{X}^*$. From (109) we see that this last condition implies that $\mathcal{E}_{\Delta x}$, $\mathcal{E}_{\Delta z}$, and $\mathcal{E}_{\Delta x} \pm \mathcal{E}_{\Delta z}$ are subsets of $\mathcal{X}^*$. Without loss of generality[5] let $x_0 = 0$, and $z_0 = 0$. Then, we have $\mathcal{E}_{\Delta x} \subset \mathcal{X}^*$ is equivalent to

$$\Delta x_{0,i} = (x_i - x_0) = x_i \in \mathcal{X}^*,\ 1 \leq i \leq L_{\mathrm{r}} - 1 \tag{119}$$

$$\Delta x_{l,i} = (x_i - x_l) \in \mathcal{X}^*,\ 1 \leq l < i \leq L_{\mathrm{r}} - 1 \tag{120}$$

Then, from (104) and (119) we get that

$$\tilde{\mathcal{E}}_x = \big\{\,\mathrm{mod}(x_i,\pi) : \{i\}_1^{L_{\mathrm{r}}-1}\big\} \subset \mathcal{X}^{**}.$$

Moreover, since (105) and (120), implies that $\mathrm{mod}(x_i,\pi) \neq \mathrm{mod}(x_l,\pi)$, $i \neq l$, then $|\tilde{\mathcal{E}}_x| = L_{\mathrm{r}} - 1$.

Similarly, employing $\mathcal{E}_{\Delta z} \subset \mathcal{X}^*$ we deduce that

$$\tilde{\mathcal{E}}_z = \big\{\,\mathrm{mod}(z_j,\pi) : \{j\}_1^{L_{\mathrm{s}}-1}\big\} \subset \mathcal{X}^{**},\ |\tilde{\mathcal{E}}_z| = L_{\mathrm{s}} - 1.$$

By the previous analysis, if only $\mathcal{E}_{\Delta x} \subset \mathcal{X}^*$ and $\mathcal{E}_{\Delta z} \subset \mathcal{X}^*$ need to be satisfied then $|\mathcal{X}^{**}| \geq \max\{L_{\mathrm{s}} - 1, L_{\mathrm{r}} - 1\}$. However, let us consider $(\mathcal{E}_{\Delta x} \pm \mathcal{E}_{\Delta z}) \subset \mathcal{X}^*$, which can be expressed as

$$(\Delta x_{l,i} \pm \Delta z_{m,j}) \in \mathcal{X}^*,\ \begin{cases} 0 \leq l < i \leq L_{\mathrm{r}} - 1 \\ 0 \leq m < j \leq L_{\mathrm{s}} - 1 \end{cases} \tag{121}$$

In particular, using $\Delta x_{0,i} - \Delta z_{0,j} = (x_i - z_j) \in \mathcal{X}^*$, which by (105) implies that

$$\mathrm{mod}(x_i,\pi) \neq \mathrm{mod}(z_j,\pi), \quad \{i\}_1^{L_{\mathrm{r}}-1}, \{j\}_1^{L_{\mathrm{s}}-1}, \tag{122}$$

we get $\tilde{\mathcal{E}}_x \cap \tilde{\mathcal{E}}_z = \emptyset$ and $|\mathcal{X}^{**}| \geq (L_{\mathrm{s}} - 1 + L_{\mathrm{r}} - 1)$. This lower bound can be further improved considering a set that contains the elements $\mathrm{mod}(x_i + z_j, \pi)$. From (121), we get that for $\{i\}_1^{L_{\mathrm{r}}-1}$, $\{j\}_1^{L_{\mathrm{s}}-1}$

$$\Delta x_{0,i} + \Delta z_{0,j} = (x_i + z_j) \in \mathcal{X}^*. \tag{123}$$

Moreover, for $\{i\}_1^{L_{\mathrm{r}}-1}$, $1 \leq m < j \leq L_{\mathrm{s}} - 1$,

$$\Delta x_{0,i} + \Delta z_{m,j} = (x_i + z_j - z_m) \in \mathcal{X}^* \overset{(105)}{\implies} \mathrm{mod}(x_i + z_j,\pi) \neq \mathrm{mod}(z_m,\pi), \tag{124}$$

$$\Delta x_{0,i} - \Delta z_{m,j} = (x_i - z_j + z_m) \in \mathcal{X}^* \overset{(105)}{\implies} \mathrm{mod}(x_i + z_m,\pi) \neq \mathrm{mod}(z_j,\pi). \tag{125}$$

Combining these last two, and since by (119) it holds that $\mathrm{mod}(x_i + z_j,\pi) \neq \mathrm{mod}(z_j,\pi)$, $\{i\}_1^{L_{\mathrm{r}}-1}, \{j\}_1^{L_{\mathrm{s}}-1}$, we deduce that $\forall i,j,n \geq 1$

$$\mathrm{mod}(x_i + z_j,\pi) \neq \mathrm{mod}(z_n,\pi). \tag{126}$$

We can use similar elaboration based on the conditions $(\Delta x_{l,i} \pm \Delta z_{0,j}) \in \mathcal{X}^*$, $1 \leq l < i \leq L_{\mathrm{r}} - 1$, and $\{j\}_1^{L_{\mathrm{s}}-1}$ to deduce that $\forall i,j,k \geq 1$

$$\mathrm{mod}(x_i + z_j,\pi) \neq \mathrm{mod}(x_k,\pi). \tag{127}$$

Finally, elaborating the conditions $(\Delta x_{l,i} \pm \Delta z_{m,j}) \in \mathcal{X}^*$, where $1 \leq l < i \leq L_{\mathrm{r}} - 1$, $1 \leq m < j \leq L_{\mathrm{s}} - 1$, and employing the fact that $\mathrm{mod}(x_i + z_j,\pi) \neq \mathrm{mod}(x_i + z_n,\pi)$, $j \neq n$, and $\mathrm{mod}(x_i + z_j,\pi) \neq \mathrm{mod}(x_k + z_j,\pi)$, $i \neq k$, we can readily reach that $\forall i,j,k,n \geq 1$, $(i,j) \neq (k,n)$

$$\mathrm{mod}(x_i + z_j,\pi) \neq \mathrm{mod}(x_k + z_n,\pi). \tag{128}$$

Now, let us gather our findings. Using (104) and (123) we deduce that

$$\tilde{\mathcal{E}}_{(x+z)} = \big\{\,\mathrm{mod}(x_i + z_j,\pi) : \{i\}_1^{L_{\mathrm{r}}-1}, \{j\}_1^{L_{\mathrm{s}}-1}\big\} \subset \mathcal{X}^{**},$$

[5] If $x_0 \neq 0$, we define $x'_0, x'_1, \cdots, x'_{L_{\mathrm{r}}-1}$ such that $x'_0 = 0$ and $x'_l = x_l - x_0$. If $z_0 \neq 0$, we analogously define $z'_0, z'_1, \cdots, z'_{L_{\mathrm{s}}-1}$. Since, $\Delta x_{l,i} = \Delta x'_{l,i}$, and $\Delta z_{m,j} = \Delta z'_{m,j}$ then $(\{x'_l\}, \{z'_m\})$ are also solutions, i.e., $\mathcal{E}_{\Delta x'} \cup \mathcal{E}_{\Delta z'} \cup (\mathcal{E}_{\Delta x'} \pm \mathcal{E}_{\Delta z'}) \subset \mathcal{X}^*$.

while (126) and (127) implies that $\tilde{\mathcal{E}}_{(x+z)} \cap (\tilde{\mathcal{E}}_x \cup \tilde{\mathcal{E}}_z) = \emptyset$, and, finally, by (128) we get that $|\tilde{\mathcal{E}}_{(x+z)}| = (L_\mathrm{s}-1)(L_\mathrm{r}-1)$.

Then, under the assumption that there exists a solution $(\boldsymbol{x}, \boldsymbol{z})$ satisfying $\mathcal{D}_X \subset \mathcal{X}^*$, we have shown that $\tilde{\mathcal{E}}_x$, $\tilde{\mathcal{E}}_z$ and $\tilde{\mathcal{E}}_{(x+z)}$ are disjoint subsets of $\mathcal{X}^{**}$, and thus

$$|\mathcal{X}^{**}| \geq L_\mathrm{r} - 1 + L_\mathrm{s} - 1 + (L_\mathrm{r}-1)(L_\mathrm{s}-1) = L_\mathrm{r}L_\mathrm{s} - 1.$$

This contradicts the claim in (118). Note that in the special case of $L_\mathrm{r} = 1$, $\mathcal{D}_X = \mathcal{E}_{\Delta z} \subset \mathcal{X}^*$, which implies $\tilde{\mathcal{E}}_z \subset \mathcal{X}^{**}$, $|\tilde{\mathcal{E}}_z| = L_\mathrm{s} - 1$, and thus $|\mathcal{X}^{**}| \geq L_\mathrm{s} - 1$. In similar manner, we can deduce that $|\mathcal{X}^{**}| \geq L_\mathrm{r} - 1$ when $L_\mathrm{s} = 1$. Both form a contradiction to (118). Therefore, we readily conclude that for $L_\mathrm{r} + L_\mathrm{s} > 2$ the statement "$\exists(\boldsymbol{x}, \boldsymbol{z}) : \mathcal{D}_X \in \mathcal{X}^* \implies L_\mathrm{r}L_\mathrm{s} \leq K$" holds, and by this we come to end the proof of the lemma. □

Now we show the claims of the theorem.

Proof. Given the objective function S_a (89), for $\boldsymbol{x} \in \mathbb{R}^{L_\mathrm{r}}$, $\boldsymbol{z} \in \mathbb{R}^{L_\mathrm{s}}$, $\boldsymbol{y} \in [0, 2\pi)^{L_\mathrm{r}}$, and $\boldsymbol{v} \in [0, 2\pi)^{L_\mathrm{s}}$, we express

$$\begin{aligned} S^\star_\mathrm{a}(\boldsymbol{\phi}) &= \sup_{\boldsymbol{x},\boldsymbol{z}} \inf_{\boldsymbol{y},\boldsymbol{v}} S_\mathrm{a}(\boldsymbol{\phi}, \boldsymbol{x}, \boldsymbol{z}, \boldsymbol{y}, \boldsymbol{v}) \\ &= K\overline{G}(\boldsymbol{\phi}) + \sup_{\boldsymbol{x},\boldsymbol{z}} \inf_{\boldsymbol{y},\boldsymbol{v}} J_\mathrm{a}(\boldsymbol{\phi}, \boldsymbol{x}, \boldsymbol{z}, \boldsymbol{y}, \boldsymbol{v}). \end{aligned} \tag{129}$$

(i) From Lemma 4 (92) we get that

$$\sup_{\boldsymbol{x},\boldsymbol{z}} \inf_{\boldsymbol{y},\boldsymbol{v}} J_\mathrm{a}(\boldsymbol{\phi}, \boldsymbol{x}, \boldsymbol{z}, \boldsymbol{y}, \boldsymbol{v}) \leq 0, \tag{130}$$

thus $S^\star_\mathrm{a}(\boldsymbol{\phi}) \leq K\overline{G}(\boldsymbol{\phi})$, and (28) follows $\big(\boldsymbol{\phi} = (\phi^\mathrm{r}, \phi^\mathrm{s})\big)$.

(ii) If $L_\mathrm{r}L_\mathrm{s} \leq K$, Lemma 6 (101) indicates that $\exists(\tilde{\boldsymbol{x}}, \tilde{\boldsymbol{z}}) : \mathcal{D}_X \subset \mathcal{X}^*$, which by Lemma 5 *(i)* implies that

$$J_\mathrm{a}(\boldsymbol{\phi}, \tilde{\boldsymbol{x}}, \tilde{\boldsymbol{z}}, \boldsymbol{y}, \boldsymbol{v}) = 0, \quad \forall \boldsymbol{y}, \boldsymbol{v}. \tag{131}$$

Hence, the upper bound in (130) is achievable, that is

$$\sup_{\boldsymbol{x},\boldsymbol{z}} \inf_{\boldsymbol{y},\boldsymbol{v}} J_\mathrm{a}(\boldsymbol{\phi}, \boldsymbol{x}, \boldsymbol{z}, \boldsymbol{y}, \boldsymbol{v}) = 0. \tag{132}$$

This, together with (129), implies that $S^\star_\mathrm{a}(\boldsymbol{\phi}) = K\overline{G}(\boldsymbol{\phi})$, hence (29) holds.

(iii) Since (132) is guaranteed when $(\tilde{\boldsymbol{x}}, \tilde{\boldsymbol{z}})$ satisfies $\mathcal{D}_X \subset \mathcal{X}^*$ then this last is a sufficient optimality condition when $L_\mathrm{r}L_\mathrm{s} \leq K$. Recalling that $x_l = \alpha^\mathrm{r}_l T/2$, $z_m = \alpha^\mathrm{s}_m T/2$, and the definition of $\mathcal{D}_X$ (96), we can straightforwardly see that $\mathcal{D}_X \subset \mathcal{X}^*$ is the same as (30), when $L_\mathrm{r} > 1, L_\mathrm{s} > 1$, while in the special cases of $L_\mathrm{r} = 1$ or $L_\mathrm{s} = 1$, it is expressed as (30b) or (30a), respectively.

(iv) Assume that (132) holds $\big($i.e., $S^\star_\mathrm{a}(\boldsymbol{\phi}) = K\overline{G}(\boldsymbol{\phi})\big)$ with solution $(\bar{\boldsymbol{x}}, \bar{\boldsymbol{z}})$. Then, for $\boldsymbol{y} \in [0, 2\pi)^{L_\mathrm{r}}, \boldsymbol{v} \in [0, 2\pi)^{L_\mathrm{s}}$

$$J_\mathrm{a}(\boldsymbol{\phi}, \bar{\boldsymbol{x}}, \bar{\boldsymbol{z}}, \boldsymbol{y}, \boldsymbol{v}) \geq \inf_{\boldsymbol{y},\boldsymbol{v}} J_\mathrm{a}(\boldsymbol{\phi}, \bar{\boldsymbol{x}}, \bar{\boldsymbol{z}}, \boldsymbol{y}, \boldsymbol{v}) = 0. \tag{133}$$

Also, by Lemma 4 (91) we get that

$$\mathcal{A}[J_\mathrm{a}(\boldsymbol{\phi}, \bar{\boldsymbol{x}}, \bar{\boldsymbol{z}}, \boldsymbol{y}, \boldsymbol{v})] = 0. \tag{134}$$

From (133) and (134), we see that over the intervals $\boldsymbol{y} \in [0, 2\pi)^{L_\mathrm{r}}$ and $\boldsymbol{v} \in [0, 2\pi)^{L_\mathrm{s}}$, the continuous function $J_\mathrm{a}(\boldsymbol{\phi}, \bar{\boldsymbol{x}}, \bar{\boldsymbol{z}}, \boldsymbol{y}, \boldsymbol{v})$ is a non-negative function that integrates to zero, and thus it must satisfy (97). It therefore, follows that (132) $\implies$ (97).

Now, given that $|g^\mathrm{r}_l(\phi^\mathrm{r})|, |g^\mathrm{s}_m(\phi^\mathrm{s})| > 0$, $\forall l, m$, then from (26) we see that $c_w, c'_w, d_u, d'_u > 0$ for $w = (l, i) \in \mathcal{P}_\mathrm{r}$, $u = (m, j) \in \mathcal{P}_\mathrm{s}$. Under these assumptions, Lemma 5 *(ii)* tells us that (97) implies that $(\bar{\boldsymbol{x}}, \bar{\boldsymbol{z}})$ satisfies $\mathcal{D}_X \subset \mathcal{X}^*$, which is again the same as (30). The condition $L_\mathrm{r}L_\mathrm{s} \leq K$, follows as an implication by Lemma 6.

(v) (Corollary 1) By Lemma 6, we know that (102), which is the same as (32), satisfies $\mathcal{D}_X \subset \mathcal{X}^*$ and thus it is optimal. Interchanging between L_r and L_s in (102), and interpreting ($x'_l = \alpha^\mathrm{s}_l T/2$, $z'_m = \alpha^\mathrm{r}_m T/2$) instead of ($x_l = \alpha^\mathrm{r}_l T/2$, $z_m = \alpha^\mathrm{s}_m T/2$) we get that (33) is also an optimal selection of phase slopes.

We have shown that all claims of Theorem 1 hold, including Remark 2 which follows from (131) and (89). Also, we have shown that the claim of Corollary 1 holds, and thus the proof is completed. □

Appendix B
Proof of Theorem 2

Proof. We start by defining, $x_l \triangleq L_\mathrm{s}\alpha^\mathrm{r}_l T/2$, $y_l \triangleq \psi^\mathrm{r}_l$, where $0 \leq l \leq L_\mathrm{r} - 1$, $e_m \triangleq |g^\mathrm{s}_m(\phi^\mathrm{s})|^2$, $0 \leq m \leq L_\mathrm{s} - 1$, and $\boldsymbol{\phi} \triangleq (\phi^\mathrm{r}, \phi^\mathrm{s})$. Then, from (39) we write J_b as

$$\begin{aligned} &J_\mathrm{b}(\boldsymbol{\phi}, \boldsymbol{x}, \boldsymbol{y}) \\ &= \sum_{m=0}^{L_\mathrm{s}-1} e_m \sum_{w \in \mathcal{P}_\mathrm{r}} c'_w \sum_{k=0}^{K_\mathrm{r}-1} \cos\big(\Delta y_w - 2\Delta x_w (m + kL_\mathrm{s})/L_\mathrm{s}\big) \\ &= \sum_{w \in \mathcal{P}_\mathrm{r}} c'_w \sum_{m=0}^{L_\mathrm{s}-1} e_m f_{K_\mathrm{r}}(\Delta x_w, \Delta y_w - 2\Delta x_w m/L_\mathrm{s}), \end{aligned} \tag{135}$$

where f_{K_r} is defined according to (73) over a sum of $K_\mathrm{r} = K/L_\mathrm{s} \in \mathbb{Z}$ terms (instead of K), $\mathcal{P}_\mathrm{r}$ is defined in (69), c'_w is defined in (26), $\boldsymbol{x} = [x_0, x_1, \cdots, x_{L_\mathrm{r}-1}]^\mathsf{T} \in \mathbb{R}^{L_\mathrm{r}}$, and $\boldsymbol{y} = [y_0, y_1, \cdots, y_{L_\mathrm{r}-1}]^\mathsf{T} \in [0, 2\pi)^{L_\mathrm{r}}$. All properties and lemmas stated for f in Appendix A-B are valid for f_{K_r}. In particular we can define a set $\mathcal{X}^*_{K_\mathrm{r}}$ according to (75),

$$\mathcal{X}^*_{K_\mathrm{r}} = \{q\pi/K_\mathrm{r} : q \in \mathbb{Z}\} \setminus \mathcal{X}, \tag{136}$$

where $\mathcal{X} = \{q\pi : q \in \mathbb{Z}\}$.

We observe that similarly to J_a (Theorem 1), J_b is also a linear combination of f_{K_r}-functions with non-negative coefficients. The arguments stated earlier to show Theorem 1 can be used here to show the result of Theorem 2. Therefore, to save on space and avoid repetition we just outline the proof steps. To show the claims of Theorem 2 we can take the following steps.

(i) Using a similar argument to what was used in Lemma 4 we can easily show that

$$\mathcal{A}_{\boldsymbol{y}}[J_\mathrm{b}(\boldsymbol{\phi}, \boldsymbol{x}, \boldsymbol{y})] = 0, \tag{137}$$

$$\inf_{\boldsymbol{y} \in [0, 2\pi)^{L_\mathrm{r}}} J_\mathrm{b}(\boldsymbol{\phi}, \boldsymbol{x}, \boldsymbol{y}) \leq 0. \tag{138}$$

where $\mathcal{A}_{\boldsymbol{y}}[h(\cdot)] = \int_{[0,2\pi)^{L_\mathrm{r}}} h(\cdot) d\boldsymbol{y}$.

(ii) By using similar steps as followed in Lemma 5, we can augment our finding by showing that
a) Given $\mathcal{D}'_X = \{\Delta x_w : w \in \mathcal{P}_\mathrm{r}\}$,

$$\mathcal{D}'_X \subset \mathcal{X}^*_{K_\mathrm{r}} \implies J_\mathrm{b}(\boldsymbol{\phi}, \boldsymbol{x}, \boldsymbol{y}) = 0, \ \boldsymbol{y} \in [0, 2\pi)^{L_\mathrm{r}}. \tag{139}$$

b) Assuming that $c'_w, e_m > 0$, $\forall w, m$ and $e_m \neq C$, $\forall m$,

$$\mathcal{D}'_X \subset \mathcal{X}^*_{K_\mathrm{r}} \Longleftarrow J_\mathrm{b}(\boldsymbol{\phi}, \boldsymbol{x}, \boldsymbol{y}) = 0,\ \boldsymbol{y} \in [0, 2\pi)^{L_\mathrm{r}}. \quad (140)$$

(iii) Last, by repeating some of the arguments used to show Lemma 6 we can show that

$$\exists \boldsymbol{x} : \mathcal{D}'_X \subset \mathcal{X}^*_{K_\mathrm{r}} \iff L_\mathrm{r} \leq K_\mathrm{r}, \quad (141)$$

and a solution that satisfies $\mathcal{D}'_X \subset \mathcal{X}^*_{K_\mathrm{r}}$ is given by

$$x_l = l\pi/K_\mathrm{r},\ l = 0, 1, \cdots, L_\mathrm{r} - 1,\ L_\mathrm{r} \leq K_\mathrm{r}. \quad (142)$$

(An alternative approach is to directly use Lemma 6 for the special case of $\hat{L}_\mathrm{s} = 1$, which implies $\mathcal{D}_X = \mathcal{D}'_X$, to prove (141) and (142).)

Then, from (39) and (42) we have that

$$S^\star_\mathrm{b}(\boldsymbol{\phi}) = K\overline{G}(\boldsymbol{\phi}) + \sup_{\boldsymbol{x} \in \mathbb{R}^{L_\mathrm{r}}} \inf_{\boldsymbol{y} \in [0, 2\pi)^{L_\mathrm{r}}} J_\mathrm{b}(\boldsymbol{\phi}, \boldsymbol{x}, \boldsymbol{y}). \quad (143)$$

The claims of Theorem (2) are shown as follows.

(i) Using (138) we deduce that $S^\star_\mathrm{b}(\boldsymbol{\phi}) \leq K\overline{G}(\boldsymbol{\phi})$.

(ii) Employing (139) and (141) we can deduce that $S^\star_\mathrm{b}(\boldsymbol{\phi}) = K\overline{G}(\boldsymbol{\phi})$ when $L_\mathrm{r} \leq K_\mathrm{r}$, and $\mathcal{D}'_X = \{\Delta x_w : w \in \mathcal{P}_\mathrm{r}\} \subset \mathcal{X}^*_{K_\mathrm{r}}$ is a sufficient optimality condition.

(iii) Given that $S^\star_\mathrm{b}(\boldsymbol{\phi}) = K\overline{G}(\boldsymbol{\phi})$ with a solution $\bar{\boldsymbol{x}}$. Then, $J_\mathrm{b}(\boldsymbol{\phi}, \bar{\boldsymbol{x}}, \boldsymbol{y}) \geq \inf_{\boldsymbol{y}} J_\mathrm{b}(\boldsymbol{\phi}, \bar{\boldsymbol{x}}, \boldsymbol{y}) = 0$. Adding this to (137), and by continuity of J_b, we deduce that $J_\mathrm{b}(\boldsymbol{\phi}, \bar{\boldsymbol{x}}, \boldsymbol{y}) = 0$, $\boldsymbol{y} \in [0, 2\pi)^{L_\mathrm{r}}$, i.e., the right-hand side of (140) holds. Now, assuming that $|g^\mathrm{r}_l(\phi^\mathrm{r})|, |g^\mathrm{s}_m(\phi^\mathrm{s})| > 0$, $\forall l, m$, and $|g^\mathrm{s}_m(\phi^\mathrm{s})| \neq C$, $\forall m$, it follows that $c'_w, e_m > 0$, $\forall w, m$ and $e_m \neq C$, $\forall m$. Then, by (140) we deduce that if $S^\star_\mathrm{b}(\boldsymbol{\phi}) = K\overline{G}(\boldsymbol{\phi})$ then $\mathcal{D}'_X \subset \mathcal{X}^*_{K_\mathrm{r}}$. The condition $L_\mathrm{r} \leq K_\mathrm{r}$ follows as a consequence of (141).

(iv) Last, since the solution in (142) satisfies $\mathcal{D}'_X \subset \mathcal{X}^*_{K_\mathrm{r}}$, then it is optimal, and by that the proof outline of the theorem is completed.

□

APPENDIX C
PROOF OF LEMMA 1

Proof. We start by defining L_s-vectors, $\boldsymbol{z} \in \mathbb{R}^{L_\mathrm{s}}$ and $\boldsymbol{v} \in [0, 2\pi)^{L_\mathrm{s}}$, with elements $z_m \triangleq \alpha^\mathrm{s}_m T/2$ and $v_l \triangleq \psi^\mathrm{s}_m$, where $0 \leq m \leq L_\mathrm{s} - 1$. Moreover, we define for every port $p = 0, 1, \cdots, P-1$, the vectors $\boldsymbol{x}^{(p)} \in \mathbb{R}^{L_{\mathrm{r},p}}$ and $\boldsymbol{y}^{(p)} \in [0, 2\pi)^{L_{\mathrm{r},p}}$, with elements $x^{(p)}_l \triangleq \alpha^\mathrm{r}_{l,p} T/2$ and $y^{(p)}_l \triangleq \psi^\mathrm{r}_{l,p}$, where $0 \leq l \leq L_{\mathrm{r},p} - 1$. Recalling that $\sum_p L_{\mathrm{r},p} = L_\mathrm{r}$, we define L_r-vector $\boldsymbol{x} = [\boldsymbol{x}^{(0)}, \boldsymbol{x}^{(1)}, \cdots, \boldsymbol{x}^{(P-1)}]^\mathsf{T} \in \mathbb{R}^{L_\mathrm{r}}$ and, similarly, we define $\boldsymbol{y} = [\boldsymbol{y}^{(0)}, \boldsymbol{y}^{(1)}, \cdots, \boldsymbol{y}^{(P-1)}]^\mathsf{T} \in [0, 2\pi)^{L_\mathrm{r}}$. Then, we can express S_d and $S_{\mathrm{a},p}$ defined in (59) and (60), respectively, as

$$\begin{aligned} S_\mathrm{d}(\boldsymbol{\phi}, \boldsymbol{x}, \boldsymbol{z}, \boldsymbol{y}, \boldsymbol{v}) &= \sum_{p=0}^{P-1} S_{\mathrm{a},p}(\boldsymbol{\phi}, \boldsymbol{x}^{(p)}, \boldsymbol{z}, \boldsymbol{y}^{(p)}, \boldsymbol{v}) \\ &= K \sum_{p=0}^{P-1} \overline{G}_p(\boldsymbol{\phi}) + \sum_{p=0}^{P-1} J_{\mathrm{a},p}(\boldsymbol{\phi}, \boldsymbol{x}^{(p)}, \boldsymbol{z}, \boldsymbol{y}^{(p)}, \boldsymbol{v}), \end{aligned} \quad (144)$$

where $\boldsymbol{\phi} = (\phi^\mathrm{r}, \phi^\mathrm{s})$, and $\overline{G}_p$, $J_{\mathrm{a},p}$ are expressed based on $\overline{G}$ (23) and J_a (25), with L_r substituted by $L_{\mathrm{r},p}$ and g^r_l by $g^\mathrm{r}_{l,p}$. In particular, $J_{\mathrm{a},p}$ can be expressed based on J_a (90), where $\mathcal{P}_\mathrm{r}$ is defined with respect to $L_{\mathrm{r},p}$ instead of L_r ($\boldsymbol{x}^{(p)}$ and $\boldsymbol{y}^{(p)}$ have $L_{\mathrm{r},p}$ elements), and c_w, c'_w, d_u, d'_u are attributed an additional sub-index p. Note that J_a and $J_{\mathrm{a},p}$ represent the same function, and the difference between the two is in notation. Using Lemma 4 (91), and recalling (67) we get that

$$\int_{\mathcal{I}} J_{\mathrm{a},p}(\boldsymbol{\phi}, \boldsymbol{x}^{(p)}, \boldsymbol{z}, \boldsymbol{y}^{(p)}, \boldsymbol{v}) d\boldsymbol{y}^{(p)} d\boldsymbol{v} = 0,\ \forall p \quad (145)$$

where $\mathcal{I} = [0, 2\pi)^{L_{\mathrm{r},p} + L_\mathrm{s}}$. Then, by the linearity of integral we can easily deduce that

$$\int_{\mathcal{J}} \sum_{p=0}^{P-1} J_{\mathrm{a},p}(\boldsymbol{\phi}, \boldsymbol{x}^{(p)}, \boldsymbol{z}, \boldsymbol{y}^{(p)}, \boldsymbol{v}) d\boldsymbol{y} d\boldsymbol{v} = 0, \quad (146)$$

where $\mathcal{J} = [0, 2\pi)^{L_\mathrm{r} + L_\mathrm{s}}$, $\sum_p L_{\mathrm{r},p} = L_\mathrm{r}$. Finally, by monotonicity of Riemann integral and (146) we can conclude that for $\boldsymbol{x} \in \mathbb{R}^{L_\mathrm{r}}$, $\boldsymbol{z} \in \mathbb{R}^{L_\mathrm{s}}$

$$\inf_{\boldsymbol{y} \in [0, 2\pi)^{L_\mathrm{r}}, \boldsymbol{v} \in [0, 2\pi)^{L_\mathrm{s}}} \left[\sum_{p=0}^{P-1} J_{\mathrm{a},p}(\boldsymbol{\phi}, \boldsymbol{x}^{(p)}, \boldsymbol{z}, \boldsymbol{y}^{(p)}, \boldsymbol{v}) \right] \leq 0,$$

which, together with (144), allows us to deduce that (63) holds, and this ends the proof of the lemma. □

REFERENCES

[1] S. Kaul, K. Ramachandran, P. Shankar, S. Oh, M. Gruteser, I. Seskar, and T. Nadeem, "Effect of antenna placement and diversity on vehicular network communications," in *Proc. 4th Annu. IEEE Commun. Soc. Conf. on Sensor, Mesh and Ad Hoc Commun. and Netw.*, pp. 112–121, June 2007.

[2] L. Ekiz, A. Posselt, O. Klemp, and C. F. Mecklenbräuker, "Assessment of design methodologies for vehicular 802.11p antenna systems," in *Proc. Int. Conf. Connected Vehicles and Expo (ICCVE)*, pp. 215–221, Nov. 2014.

[3] O. Klemp, "Performance considerations for automotive antenna equipment in vehicle-to-vehicle communications," in *Proc. URSI Int. Symp. on Electromagn. Theory*, pp. 934–937, Aug. 2010.

[4] K. K. Nagalapur, E. G. Ström, F. Brännström, J. Carlsson, and K. Karlsson, "Robust connectivity with multiple directional antennas for vehicular communications," *IEEE Trans. Intell. Transp. Syst.*, vol. 20, pp. 5305–5315, Dec. 2020.

[5] S. Kaul, M. Gruteser, V. Rai, and J. Kenney, "Minimizing age of information in vehicular networks," in *Proc. IEEE Commun. Soc. Conf. on Sensor, Mesh and Ad Hoc Commun. and Netw.*, pp. 350–358, June 2011.

[6] C. B. Lehocine, E. G. Ström, and F. Brännström, "Hybrid combining of directional antennas for periodic broadcast V2V communication," *IEEE Trans. Intell. Transp. Syst.,* early access, Nov. 2020, doi: 10.1109/TITS.2020.3033094.

[7] M. Larsson, M. Jonsson, K. Karlsson, C. Bergenhem, and T. Larsson, "Curvature based antenna selection method evaluated using the data age metric and V2V measurements," in *Proc. IEEE Int. Conf. on Commun. Workshop (ICCW)*, pp. 2356–2362, June 2015.

[8] S. Roger, D. Martn-Sacristn, D. Garcia-Roger, J. F. Monserrat, A. Kousaridas, P. Spapis, and S. Ayaz, "5G V2V communication with antenna selection based on context awareness: Signaling and performance study," *IEEE Trans. on Intell. Transp. Syst.,* early access, Sept. 2020, doi: 10.1109/TITS.2020.3019530.

[9] S. Zhang, C. Guo, T. Wang, and W. Zhang, "ONOFF analog beamforming for massive MIMO," *IEEE Trans. on Veh. Technol.*, vol. 67, no. 5, pp. 4113–4123, 2018.

[10] X. Yang, W. Jiang, and B. Vucetic, "A random beamforming technique for omnidirectional coverage in multiple-antenna systems," *IEEE Trans. on Veh. Technol.*, vol. 62, pp. 1420–1425, Nov. 2013.

[11] S. M. Alamouti, "A simple transmit diversity technique for wireless communications," *IEEE J. on Sel. Areas in Commun.*, vol. 16, pp. 1451–1458, Oct. 1998.

[12] T. Abbas, J. Karedal, F. Tufvesson, A. Paier, L. Bernado, and A. F. Molisch, "Directional analysis of vehicle-to-vehicle propagation channels," in *Proc. IEEE 73rd Veh. Technol. Conf. (VTC Spring)*, July 2011.
[13] A. F. Molisch, *Wireless Communication*. Wiley, 2nd ed., 2011.
[14] D. Tse and P. Viswanath, *Fundamentals of Wireless Communication*. Cambridge University Press, 2004.
[15] *Intelligent Transport Systems Vehicular Communications; Basic Set of Applications; Part 2: Specification of Cooperative Awareness Basic Service,* document ETSI EN 302 637-2 V1.3.2, Nov. 2014.
[16] J. Daniel, C. Qi, and D. Luca, "Optimal data rate selection for vehicle safety communications," in *Proc. of the 5th ACM Int. Workshop on Veh. Inter-Networking*, pp. 30–38, Sept. 2008.
[17] M. E. Renda, G. Resta, P. Santi, F. Martelli, and A. Franchini, "IEEE 802.11p VANets: Experimental evaluation of packet inter-reception time," *Comput. Commun.*, vol. 75, pp. 26–38, 2016.
[18] L. Bernad, T. Zemen, F. Tufvesson, A. F. Molisch, and C. F. Mecklenbruker, "Time- and frequency-varying K-factor of non-stationary vehicular channels for safety-relevant scenarios," *IEEE Trans. on Intell. Transp. Syst.*, vol. 16, pp. 1007–1017, April 2015.
[19] Q. Liu, S. Zhou, and G. Giannakis, "Cross-layer combining of adaptive modulation and coding with truncated ARQ over wireless links," *IEEE Trans. on Wireless Commun.*, vol. 3, pp. 1746–1755, Oct. 2004.
[20] A. Stamoulis and N. Al-Dhahir, "Impact of space-time block codes on 802.11 network throughput," *IEEE Trans. on Wireless Commun.*, vol. 2, pp. 1029–1039, Sept. 2003.
[21] *IEEE Standard for Information technology—Telecommunications and information exchange between systems Local and metropolitan area networks—Specific requirements–Part 11: Wireless LAN Medium Access Control (MAC) and Physical Layer (PHY) Specifications–Amendment 4: Enhancements for Very High Throughput for Operation in Bands below 6 GHz,* IEEE Standard 802.11ac-2013, Dec. 2013.
[22] M. Marey and H. Mostafa, "Maximum-likelihood integer frequency offset estimator for Alamouti SFBC-OFDM systems," *IEEE Commu. Letters*, vol. 24, pp. 777–781, April 2020.
[23] B. Holter and G. Øien, "The optimal weights of maximum ratio combiner using an eigenfilter approach," in *Proc. 5th IEEE Nordic Signal Process. Symp. (NORSIG)*, Oct. 2002. [Online]. Available: https://www.ux.uis.no/norsig/norsig2002/proceedings.html.
[24] "Mathematical models for radiodetermination radar systems antenna patterns for use in interference analyses," *Recommendation ITU-R M1851-1*, Jan. 2018.